2012

Investigating the transcriptional regulation by OxyR in Porphyromonas gingivalis.

Anuya R. Paranjape
Virginia Commonwealth University

Investigating the transcriptional regulation by OxyR in *Porphyromonas gingivalis*

A dissertation submitted in partial fulfillment of the requirements for the degree of Masters in Science at Virginia Commonwealth University

by

Anuya R. Paranjape
B.Pharm, Bombay College of Pharmacy, India, 2010

Director: Dr. Janina P. Lewis
Associate Professor, Oral and Cranofacial Biology

Virginia Commonwealth University
Richmond, Virginia
August 2012

Acknowledgements

I would like to take this opportunity to express my gratitude to my Ph.D. mentor, Dr. Janina P. Lewis for her guidance and support over these years. I would also like to extend my heartfelt gratitude to my committee members, Dr. Henderson and Dr. Wright for guiding me through each and every phase of my thesis. Special thanks to Dr. Henderson and Ms. Francis White for spending their valuable time and helping me with fluorescence microscopy. I would also like to acknowledge Dr. Wright for his help and guidance in purifying the OxyR protein.

I would also like to thank all my lab mates, past and present for their continued support. I would specially like to thank Sai Yanamandra for showing patience while teaching me and answering my questions. CHIP-chip assay performed by her formed the basis of my project.

I would also like to take this opportunity to thank my parents, Aai and Baba and my grandmother, Aaji, for showing their confidence in me and encouraging me through these years.

Table of Contents

List of Figures

Figure 10. EMSA using mutant OxyR cell lysates, where, A – IPTG < 1 mM and B – IPTG = 1 mM. Lane 1 – DNA only, Lane 2 – DNA+ un-induced mutant C199S cell lysate, Lane 3 – DNA+ Induced mutant C199S cell lysate, Lane 4 – DNA+ un-induced mutant H17A cell lysate, Lane 5 – DNA+ Induced mutant H17A cell lysate.

Figure 11. EMSA using *in vitro* transcribed OxyR mutants with DNA fragments PG1307 (A), *hmu* (B) and PG0964 (C) where Lane 1- DNA only, Lane 2 - DNA+ Wt. OxyR, Lane 3- DNA+ mutant C199S, Lane 4- DNA+ mutant H123A.

Figure 12. SDS-PAGE gel image of the purified *P. gingivalis* OxyR and *E. coli* OxyR from batch 2, where Lane 1 – *P. gingivalis* OxyR under non-reducing conditions, Lane 2 – *E. coli* OxyR under non-reducing conditions, Lane 3 – *P. gingivalis* OxyR under reducing conditions, Lane 4 – *E. coli* OxyR under reducing conditions.

Figure 13. EMSA using fresh purified wild type *P. gingivalis* OxyR and *E. coli* OxyR with different DNA fragments.
A. Lane 1 – IGS DNA only, Lane 2 – IGS DNA + IGS protein treated with hemin, Lane 3 – IS DNA only, Lane 4 – IS DNA + *E. coli* OxyR, Lane 5 – IS DNA + *P. gingivalis* OxyR, Lane 6 – PG ahpc1 DNA only, Lane 7 - PG ahpc1 DNA + *E. coli* OxyR, Lane 8 - PG ahpc1 DNA + *P. gingivalis* OxyR, Lane 9 – PG ahpc2 DNA only, Lane 10 – PG ahpc2 DNA + *E. coli* OxyR, Lane 11 - PG ahpc2 DNA + *P. gingivalis* OxyR, Lane 12 – *hmu* DNA only, Lane 13 – *hmu* DNA + *E. coli* OxyR Lane 14 - *hmu* DNA + *P. gingivalis* OxyR
B. Lane 1 – PG0964 DNA only, Lane 2 - PG0964 DNA + *E. coli* OxyR, Lane 3 - PG0964 DNA + *P. gingivalis* OxyR, Lane 4 – PG0360 DNA only + Lane 5 – PG0360 DNA + *E. coli* OxyR, Lane 6 - PG0360 DNA + *P. gingivalis* OxyR.

Figure 14. EMSA using equal concentrations of purified wild type *P. gingivalis* OxyR and *E. coli* OxyR with different DNA fragments.
A. Lane 1 – IGS DNA only, Lane 2 – IGS DNA + IGS protein treated with hemin, Lane 3 - IGS DNA + IGS untreated protein, Lane 4 – IS DNA only, Lane 5 – IS DNA + *E. coli* OxyR, Lane 6 – IS DNA + *P. gingivalis* OxyR, Lane 7 – PG ahpc1 DNA only, Lane 8 - PG ahpc1 DNA + *E. coli* OxyR, Lane 9 - PG ahpc1 DNA + *P. gingivalis* OxyR, Lane 10 – PG ahpc2 DNA only, Lane 11 – PG ahpc2 DNA + *E. coli* OxyR, Lane 12 - PG ahpc2 DNA + *P. gingivalis* OxyR, Lane 13 – *hmu* DNA only, Lane 14 – *hmu* DNA + *E. coli* OxyR Lane 15 - *hmu* DNA + *P. gingivalis* OxyR (Refer tables .. and … for details regarding DNA fragments).
B. Lane 1 – PG0964 DNA only, Lane 2 - PG0964 DNA + *E. coli* OxyR, Lane 3 - PG0964 DNA + *P. gingivalis* OxyR, Lane 4 – PG0360 DNA only + Lane 5 – PG0360 DNA + *E. coli* OxyR, Lane 6 - PG0360 DNA + *P. gingivalis* OxyR.

Figure 15 A. DIC (Differential interference contrast) images of the live cell microscopy experiment to monitor OxyR expression in real time captured on *Zeiss Cell Observer Spinning Disc Microscope* after every 15 minutes, starting from 0 minute to 5 hours.

Figure 15 B. Overlay of DIC + fluorescence images from the live cell microscopy experiment to monitor OxyR expression in real time captured on *Zeiss Cell Observer Spinning Disc Microscope* after every 15 minutes, starting from 0 minute to 5 hours.

Figure 16. Agarose gel showing plasmid DNA V3080 (Lane 1) and the re-constructed pUC18 vector (Lane 2) digested with Xhoi, EcoRi.

Figure 17A. Agarose gel to check the amplification of pGLOW-Bs2 inserts, where Lane 1, 2 – Inserts amplified with primer pair FP1-RP, Lanes 3 – Insert amplified with primer pair FP2-RP.

Figure 17B. Vectors V3080 (lane 1) and V3107 (lane 2) digested with Xhoi and EcoRi

Figure 18A. Sequencing result obtained after cloning pGLOW-Bs2 downstream *P. gingivalis* OxyR present in Flexi vector where blue, bold letters indicate the end part of the sequence of *P. gingivalis* OxyR

Figure 18B. Sequencing result obtained after cloning pGLOW-Bs2 downstream *E. coli* OxyR present in Flexi vector where blue, bold letters indicate the end part of the sequence of *E. coli* OxyR

Figure 19A. Sequence of vector P1 (Bs2 amplified with primer pair FP1-RP cloned in TOPO2.1 PCR vector), where Green, bold, underlined letters - the sequence of Bs2, Pink, bold, underlined letters - recognition sequences of Xhoi, EcoRi, Dark pink, bold, underlined letters – sequence for *E. coli* RBS, Red, bold, underlined letters – stop codon, pink letters – primer sequences, Black letters- sequence from TOPO vector.

Figure 19B. Sequence of vector P2 (Bs2 amplified with primer pair FP2-RP cloned in TOPO2.1 PCR vector), where Green, bold, underlined letters - the sequence of Bs2, Pink, bold, underlined letters - recognition sequences of Xhoi, EcoRi, Dark pink, bold, underlined letters – sequence for *P. gingivalis* RBS, Red, bold, underlined letters – stop codon, pink letters – primer sequences, Black letters- sequence from TOPO vector.

Figure 20A. Vectors V3080 (lane 1) and V3107 (lane 2) again digested with Xhoi and EcoRi.

Figure 20B. Construct P1 (lane 1) and construct P2 (Lane 2) digeted with Xhoi and EcoRi.

Figure 21A. Sequence of construct ***P*** where, where Blue, blue letters – Sequence from the end part of *E. coli* OxyR, Green, bold, letters - the sequence of Bs2, Pink, bold, underlined letters - recognition sequences of Xhoi, EcoRi, Dark pink, bold, underlined letters – sequence for *E. colis* RBS, Red, bold, underlined letters – stop codon, pink letters – primer sequences, Black letters- sequence from Flexi vector.

Figure 21B. Sequence obtained while making construct ***Q*** where, where Blue, blue letters – Sequence from the end part of *P. gingivalis* OxyR, Green, bold, letters - the sequence of Bs2, Pink, bold, underlined letters - recognition sequences of Xhoi, EcoRi, Dark pink, bold,

underlined letters – sequence for *E. coli* RBS, Red, bold, underlined letters – stop codon, pink letters – primer sequences.

Figure 21C. Sequence obtained while making construct ***R*** where, Blue, blue letters – Sequence from the end part of *P. gingivalis* OxyR, Green, bold, letters - the sequence of Bs2, Pink, bold, underlined letters - recognition sequences of Xhoi, EcoRi, Dark pink, bold, underlined letters – sequence for *P. gingivalis* RBS, Red, bold, underlined letters – stop codon, pink letters – primer sequences.

Figure 22. Sequencing result of the positive control vector constructed using Flexi vector, where green letters – sequence encoding pGLOW-Bs2, red letters – stop codon, black letters – sequence from the Flexi vector.

Figure 23. Images captured to check fluorescence after expression from construct pGLOW-Bs2-K^{XN}-Bs2 and from construct V3080 (negative control).

List of abbreviations

1. ROS – Reactive oxygen species
2. MALDI-TOF – Matrix-assisted laser desorption/ionization-Time of Flight
3. *Grx1 – Glutaredoxin A*
4. bp – base pairs
5. EMSA – Electrophoretic Mobility Shift Assay
6. LB media – Lysogeny broth / Luria-Bertani medium.
7. NEB – New England Biolabs
8. *PG –Porphyromonas gingivalis*
9. *EC – E. coli*
10. CHIP- Chromatin immuno precipitation
11. kDa – kilo Dalton
12. IPTG – Isopropyl β-D-1-thiogalactopyranoside
13. PAGE – Polyacrylamide gel electrophoresis
14. DTT – Dithiothreitol
15. LB broth – Lysogeny broth
16. *ahpC - alkyl hydroperoxidase C*
17. catalase – *katG*
18. *dps* – non specific DNA binding protein
19. *gorA* - glutathione reductase
20. *sod – superoxide dismutase*
21. *trxA* - thioredoxin

Abstract

Investigating the transcriptional regulation by OxyR in *Porphyromonas gingivalis*

A dissertation submitted in partial fulfillment of the requirements for the degree of Masters in Science at Virginia Commonwealth University

by

Anuya R. Paranjape
B.Pharm, Bombay College of Pharmacy, India, 2010

Director: Dr. Janina P. Lewis
Associate Professor, Oral and Cranofacial Biology

Periodontal diseases are bacterially induced, inflammatory diseases which are responsible for loss of alveolar bone and connective tissue supporting the teeth which results in loss of teeth. Gram negative anaerobic bacteria are highly associated with these diseases. One of them is *Porphyromonas gingivalis* belonging to the phylum *Bacteroidetes*. Infection by *P. gingivalis* is recurrent after physical removal of the bacteria from the oral cavity and even after antibiotic treatment as development of resistance is not rare. Hence complete understanding the biology of this bacterium is of significance.

This gram negative obligate anaerobe, being aerotolerant, manages to survive inside the oral cavity, where oxidative stress is ubiquitous. Genome sequence of *P. gingivalis* shows the presence of a transcriptional regulator OxyR which is a homologue of OxyR present in *E. coli*. *P. gingivalis* OxyR induces the expression of antioxidant defense genes like *sod, ahpC-F, dps* to

protect the bacteria from oxidative stress. Expression of *P. gingivalis* OxyR regulon is not very well understood.

Microarray studies carried out in our lab using *P. gingivalis* W83 to study gene regulation by OxyR, indicated that several genes in *P. gingivalis* are co-regulated by iron-and OxyR. Literature also supports that in iron deplete conditions genes involved in oxidative stress are down-regulated. These studies formed the basis of our hypothesis that OxyR might regulate the genes in *P. gingivalis* in an iron dependent manner.

To study the mechanism of regulation by *P. gingivalis* OxyR and to determine whether OxyR regulation is iron dependent, two approaches were applied - *in vitro* characterization of binding and *in vivo* characterization.

First step of *in vitro* characterization was to perform CHIP-chip assay to determine OxyR-binding sites present on the genomic DNA of *P. gingivalis*. As this assay was performed under completely anaerobic conditions, the target fragments to which OxyR was found to bind during this assay were not same as reported in literature. These and the fragments reported in literature were used for EMSA. EMSAs carried out using crude cell lysates and in vitro OxyR protein preparations showed expected results but the results were not reproducible. *In vivo* expressed and purified *P. gingivalis* OxyR never bound to the target fragments used. Preparation of a stable protein preparation and improvement in the parameters of EMSA is very important to further investigate the binding *in vitro*.

The second approach is based on *in vivo* characterization of binding. This requires tagging the *P. gingivalis* OxyR at its C-terminus with fluorescent protein to observe its binding to the target DNA sequences. Fluorescently tagged OxyR, is expected to emit fluorescence from a highly localized area to produce sharp fluorescent spots when it is bound to its target sequences.

Unbound OxyR is expected to emit a fluorescent signal which is spread over the entire area of the cell. This technique will help to determine the conditions under which OxyR binds to its target DNA sequences. This provides a means to confirm the results obtained from in vitro characterization instead of just extrapolating them.

1.1. Introduction

Drawing analogy to the human body, oral cavity has its own natural micro-flora[1-3]. All dental and mucosal surfaces are colonized by diverse pathogenic and non-pathogenic microorganisms[4]. The oral cavity comprising of the teeth, gingival sulcus, attached gingiva, tongue, cheek, lip, hard and soft palate have various distinct habitats of microorganisms[5]. The natural micro-flora has a specific composition that varies for different sites in the oral cavity due to differences in prevailing biological conditions[4]. Studies document the presence of 500 to 700 common oral species and *culture independent molecular methods* have identified 600 different species or phenotypes[4]. Studies have identified the presence of specific bacterial strains representing mainly six bacterial phyla in the oral cavity namely, the *Firmicutes* (species of *Gemella, Streptococcus, Eubacterium, Selenomonas* and *Veillonella*), *Actinobacteria* (species of *Actinomyces, Atopobium, Rothia*), *Proteobacteria* (species of *Neisseria, Eikenella, Campylobacter*), *Bacteroidetes* (Species of *Porphyromonas, Prevotella, Capnocytophaga*), *Fusobacteria* (species of *Fusobacterium, Leptotrichia*) and the *TM7* phylum. Some species like *Gemella, Granulicatella, Streptococcus* and *Veillonella* reside in most of the sites in the oral cavity while some strains are very site specific[3].

As mentioned earlier, this plethora of microorganisms encompass both essential and pathogenic organisms. Beneficial effects of some oral bacterial strains include contribution towards the maintenance of gastrointestinal and cardiovascular health via metabolism of dietary nitrate to nitrite by reduction[6]. Evidences indicate the existence of a cross-talk between some of resident bacteria and cells of the oral mucosa, which contribute towards down regulating the potentially damaging pro-inflammatory host responses to normal microflora[7,8]. Whereas, certain microorganisms residing the oral cavity are responsible for a number of infectious diseases,

involving caries (tooth decay), periodontitis (gum disease), endodontic infections (root canal), alveolar osteitis (dry socket) and tonsillitis. Studies have revealed that most of these infections are caused by a consortia of microorganisms[5]. It has also been observed that individuals experiencing a good oral health do not exhibit a complete absence of infectious organisms, hence presence or absence of a particular organism is not clear indication of the onset of disease. Diseases are initiated either due to change in the relative or absolute numbers of pathogenic and beneficial organisms or due to modulation of host factors which result in loss of harmony between the organism and the host[9].

1.1.1. Periodontitis. One of the most common oral diseases is periodontitis[3]. It has been estimated that at least 35% of dentate U.S adults aged 30 to 90 years suffer from periodontitis[10]. Periodontitis is a set of inflammatory disease affecting the periodontum that includes periodontal tissues surrounding and supporting the teeth. The periodontum is made up of four tissues, namely, the gingiva (gum tissue), cementum (outer tissues of the roots of teeth), alveolar bone (sockets where the teeth are anchored) and periodontal ligaments (connective tissues joining the cementum and the alveolar bone). Periodontitis is marked by the infection of periodontal ligament fibers and alveolar bone supporting the teeth, which ultimately leads to loosening and loss of teeth[11]. Poor oral hygiene leading to accumulation of mycoses and bacterial biofilms at the gum line account for the primary etiology of periodontitis[12-14]. Periodontitis lesions are usually accompanied with gingival redness and swelling. The onset of periodontitis may occur through gingival inflammations, however all gingivitis lesions do not lead to periodontitis[15].

Visual detection of gingival changes is suggestive of periodontitis but often misleading since periodontitis is not always accompanied by physiological changes in the gingiva. Early symptoms suggesting the onset of periodontitis involve bleeding on probing (BOP), pocket

probing depth (PPD), clinical attachment loss (CAL) and radiographically assessed alveolar bone loss[16], among which PPD and CAL are the most common techniques. Apart from oral infections, periodontitis has been associated with an increased inflammation of the body observed by raised levels of C-reactive protein and Interleukin-6 (IL-6)[17-19]. This disease also leads to memory impairment[20,21] for older patients and furthermore has been linked to an increase in susceptibility to myocardial infarction[22], artherosclerosis[23,24] and an increased risk of stroke[22]. Individuals with impaired fasting glucose (IFG) and diabetes mellitus have a higher degree of periodontal inflammation which leads to a constant elevated blood glucose level due to the constant systemic inflammation[25,26].

The etiology of periodontal diseases have been the subject of investigation for almost a century[27-29]. Two fundamental schools of thought are prevalent in the literature where, one proposed bacterial plaques as the cause of periodontitis whereas the other suggested bacterial colonization to be a secondary event[30]. Over the past few decades, studies have shown the role of dental plaque organisms in the etiology of periodontitis[31], where a positive correlation was established between the severity of periodontal disease and the amount of dental plaque. Clinical studies on humans and experimental animals have demonstrated the presence of bacterial plaques prior to periodontal infection[32-34]. Furthermore, a microbial concentration dependant periodontal infection provided additional proof of the theory[35].

1.1.2. Causative Microbes and P. gingivalis. It has been observed that a wide range of microbes are responsible for initiation of periodontal diseases but generally more severe forms of the disease in adults are observed to be associated with the increased number of Gram negative anaerobic bacteria[9]. Statistical studies performed on healthy and diseased individuals are in compliance with this observation, pointing towards *B. forsythus*, *P.gingivalis, T. denticola*, and *S.*

noxia as potential periodontal pathogens[10]. Among the array of Gram negative bacteria, evidences for most pathogenicity has been observed for *Porphyromonas gingivalis*.

P. ginigivalis, is a Gram negative, obligate anaerobic bacterium[36]. *P. gingivalis* is considered to be the causative agent in 37 to 63% of juvenile periodontitis, whereas it accounts for 40 to 100% of periodontitis occurring in adults. *P. gingivalis* forms a higher fraction of the oral microbiota in deep periodontal pockets[37]. This pathogen can adhere to the oral cavity like teeth, oral mucosa and other oral bacteria through its long, filamentous structures called fimbrae[38]. *P. gingivalis* is a late or secondary colonizer of oral cavity where it depends on antecedent organisms which create the necessary environment for colonization of *P.gingivalis*[9]. Studies have shown that highly virulent *P. gingivalis* strains cause severe tissue damage and even death, whereas less virulent ones have a milder effect on periodontal tissues. The presence of the organism at inaccessible areas of the oral cavity makes it difficult for eradication through mechanical techniques. Bacteria rapidly develop resistance to antibiotics. Infections are recurrent even after antibiotic treatment. Hence more targeted and longer-lasting approaches are needed to reduce colonization of *P. gingivalis* in the oral cavity. For that a complete understanding of the biology of *P. gingivalis* is necessary[39].

The predominant role played by *P. gingivalis* in adult periodontitis together with their virulent pathogenicity are the main reasons for designating them as prime pathogens for adult periodontitis. Virulence differs among various strains of *P. gingivalis.* Studies on the association of individual hetero-duplex types of *P. gingivalis* with periodontitis were analyzed and strain W83 was statistically found to be highly associated with the disease. While both healthy individuals as well as individuals with periodontitis harbor multiple strains, their distribution is different among these two groups of people. The virulent strains present in individuals with

periodontitis are likely to dominate the ecological niche and inhibit the colonization of less virulent strains[38]. Since *P. gingivalis* is an opportunistic pathogen, it is also true that virulence is not restricted to a particular clonal type[9]. To sum up, periodontal diseases range in severity, rate of progression of the disease, causative organisms involved, number of affected teeth and the susceptible age-group[9]. Our research group is working on *P. gingivalis* strain W83, which is fully sequenced and is believed to be the most virulent strain.

1.1.3. LysR type transcriptional regulator (LTTR). LTTR is the largest known, highly conserved family of prokaryotic DNA binding proteins consisting of 800 members[40]. The members of this family are identified on the basis of their amino acid sequences[41]. The transcriptional activator LysR is a well studied and the best characterized member of this family. It activates the expression of a divergently transcribed *lysA* gene in *E. coli,* negatively regulating its own expression[42]. Since the discovery of *lysA*, many more LTTRs have been identified. Members of this group belong to extremely diverse groups of bacteria and regulate genes with diverse functions like metabolism, cell division, quorum sensing, virulence, motility, nitrogen fixation, oxidative stress responses, toxin production, attachment and secretion[40,41]. In spite of this diversity, important structural regions remain highly conserved among the family members. LTTRs are made up of approximately 330 amino acids having helix-turn-helix (HTH) motif at the N-terminus for DNA binding site among which residues 20 to 80 are the most highly conserved. The C terminus of these proteins is composed of α/β subdomains connected through a hinge/cleft[40] which is believed to accommodate a co-inducer[43]. The C terminus has a co-factor binding domain which helps the proteins to interact with DNA at their major groove. Comparatively less conservation at the amino acid level is observed at the C terminus of LTTRs.

Studies have shown that LTTRs exhibit negative auto-regulation. Initially these proteins were believed to be the transcriptional activators of a single, divergently transcribed gene, though some of them showed repressor like effects for some promoters[41]. Over the years, research work has proved that LTTRs can behave as either activators or repressors of operonic genes. Although these proteins mostly regulate transcription of divergently transcribed genes, those located elsewhere on the bacterial chromosome could also be regulated[44,45]. LTTRs protect unusually long regions of DNA from DNase1 digestion suggesting that these are multimeric nature of these proteins.

1.1.4. Reactive oxygen species (ROS). These moieties are generated during a number of cellular processes some of which include incomplete reduction of oxygen during respiration, radiation exposure and release from macrophages in response to microbial invasion[46]. It has been observed that cellular redox homeostasis is dependent on the concentration of intracellular ROS[47]. ROS can have damaging effects on intracellular DNA, proteins, lipids membranes and are responsible for initiation of many degenerative processes like DNA damage and mutations[47,48]. Generally, cells respond to increased levels of ROS through proteins whose activities are regulated by oxidation and one such representative protein that has been well documented in the literature is OxyR[47,48]. OxyR protein present in a facultative anaerobic bacteria, *Escherichia coli*, has been well studied over the past few decades[48].

1.1.5. E. coli OxyR. OxyR in *E. coli* is a transcriptional regulator belonging to the LTTR family[48]. This 34 KDa protein[49] acts as a transcriptional inducer for genes involved in bacterial defense against oxidative stress[47,48]. In response to increased concentration of intracellular hydrogen peroxide, OxyR rapidly activates the transcription of *OxyS* (a small, non-translated regulatory RNA), *katG* (hydrogen peroxidase I), *gorA* (glutathione reductase), *grxA*

(glutaredoxin A) , *ahpC* (alkyl hydroperoxidase C) and *dps* (non-specific DNA binding protein)[48,50]. It has been observed from prior studies that OxyR can negatively regulate its own expression[49]. To investigate the mechanism of OxyR regulation, studies were carried out to determine whether this increase in transcription of target genes was due to increased levels of OxyR protein within the bacterial cell. Neither the total amount of OxyR nor its synthesis increased significantly after peroxide treatment, suggesting that a modification in the pre-existing OxyR is responsible for elevated expression of the *oxyR* regulon. Further studies proved that the capacity of OxyR to activate transcription is directly dependent on its redox state, the oxidized form being the only transcriptionally active form[48].

The intracellular environment in prokaryotic and eukaryotic cells is reducing in nature. Studies have shown the redox potential of *E. coli* cytosol to be approximately -0.26 to -0.28 volts[47,51]. Hence protein disulphide bonds do not occur frequently[47,51]. Hence, under normal circumstances intracellular OxyR exists in its reduced (inactive) form. Only when the intracellular redox homeostasis gets disrupted due to increased concentration of hydrogen peroxide, OxyR gets converted into oxidized (active) form[48]. The two forms, oxidized (active form) and reduced (inactive form), are readily and rapidly interconvertible[48].

Oxidized as well as reduced OxyR binds to the promoters of its target genes with high affinity suggesting that the reason for transcriptional activation by only the oxidized form is not due to greater affinity for DNA binding by oxidized form. In fact, it is postulated that low concentrations of reduced form of OxyR bound to *oxyR* promoters are always present intra-cellularly. A conformational change due to oxidation in the OxyR that is already bound to its promoters is responsible for activation. This hypothesis is further established by the difference in

the lengths of the OxyR footprint under oxidizing and reducing conditions, elucidated in the subsequent sections[48].

Being a member of the LysR family, OxyR possesses a HTH domain at its N-terminus which was proposed to be directly involved in DNA binding and a C-terminal regulatory domain. Random mutagenesis studies on OxyR, in which five out of the six mutations that caused DNA binding defect mapped near the conserved helix-turn-helix motif proved the role of N-terminal domain in DNA-binding[52]. A truncated version of OxyR in which 22 amino acids were deleted, was not capable to function as a regulator indicating that C terminus may also be critical for binding[52]. Random mutagenesis studies showed that the residues important for oligomerization are located in the C-terminal domain[52].

Crystal structures of the regulatory domain of OxyR in oxidized and reduced form are analyzed[47]. Gel retardation assays showed that OxyR is a tetramer in solution[52]. The structural features critical for conversion from reduced to oxidized form were well investigated. Presence of chelators does not affect the capacity of OxyR to activate transcription[48]. Studies suggest that it is unlikely for metals ions and other prosthetic groups to be the redox-active center of OxyR[47]. Mutational studies pointed towards Cys 199 and Cys 208 as redox active centers[47,52]. Site directed mutagenesis studies proved that mutation C199S locks OxyR in reduced state[52]. Assays based on MALDI-TOF and quantitative thiol-disulphide titrations indicated that OxyR is oxidized due to formation of an intramolecular disulphide bond between these two active cystein residues[47,53]. Wild type and C199S mutant protein have the same conformation on a non-reducing gel, suggesting that intermolecular disulphide bridges do not form redox active centers, confirming the presence of intramolecular disulphide bonds[47]. Oxidation of OxyR starts with the

initial oxidation of Cys 199 to form a sulphenic acid intermediate which indicates that residues Cys 199 and Cys 208 are not equivalent[54-56].

Structure of the regulatory domain undergoes a significant change when disulfide bond is formed. ROS-mediated redox switch is present in each monomer of OxyR. It leads to changes in oligomeric interfaces. Fold modifications leading to different tetrameric orientations of OxyR result in reorientation of OxyR relative to the DNA. This also could result in presentation of RNA polymerase contact sites in an orientation that is favorable to transcriptional activation[47].

OxyR binds upstream of the promoters it regulates. DNase I footprints for OxyR are 45 bp long[57,58]. Studies on seven natural binding sites showed limited homology leading to a conclusion that 'OxyR may have a degenerate recognition code'[57,58]. Analysis of 54 synthetic binding sites allowed researchers to define a consensus binding motif (ATAGntnnnanCTATnnnnnnnATAGntnnnanCTAT) for oxidized OxyR. These studies suggested that OxyR-DNA binding is based on a specific recognition code[58].

Hydroxyl radical footprinting and interference assays also showed that the oxidized OxyR tetramer binds to the four ATAGxt elements by contacting the DNA in four adjacent major grooves. As the key nucleotides are found to be dispersed and both the natural and synthetic sites diverge from the consensus motif, it is proposed that OxyR achieves tight, specific binding through the four contacts of intermediate affinity[58].

Footprint of reduced OxyR is longer that that for oxidized OxyR[47] indicating that binding of OxyR is distinct in oxidized and reduced conditions[58]. Reduced OxyR contacts two pairs of adjacent major grooves separated by one helical turn. In short, whether oxidized or reduced, OxyR tetramer contacts DNA at four regions of intermediate affinity. In each region it contacts

one to three nucleotides. As cellular redox state changes, OxyR repositions its DNA contacts and targets alternate sets of promoters[58].

OxyR acts as a transcriptional activator of oxidative stress defense genes only for a limited period of time [48,59] as activation of OxyR to oxidized state is a transient phenomenon[48]. Genetic and biochemical studies proved that deactivation of OxyR takes place primarily by enzymatic reduction by Grx1. The expression of Grx1 and glutathione reductases is induced by oxidized OxyR itself. This autoregulation helps to maintain cellular redox balance. Other reduction systems also may contribute in vivo[48]. The process of reduction is slower than the oxidation enabling the oxidized OxyR to stay for an extended time under the overall reducing environment inside the *E. coli* cells[60].

Though, diamide and S-nitroso-Cysteine can react with the two redox active cysteins of OxyR, it specifically senses peroxides[47]. Findings uptill now suggested that OxyR is the sole sensor and transducer of oxidative stress in *E. coli*[48]. In contrast to this, some recent studies stated that endogenous protein S-Nitrosylation in *E. coli* is under OxyR regulation[61].

1.1.6. P. gingivalis OxyR. *P. gingivalis* is an example from the class of obligate anaerobic bacteria. During transmission from host to host, *P. gingivalis* being a periopathogen, is exposed to atmospheric oxygen, which is the case during their survival in saliva[62,63]. During this journey, unfavorable redox potential and damaging effects of ROS might challenge the survival of *P. gingivalis*. This situation prevails even after *P. gingivalis* becomes a part of the subgingival biofilm. *Streptococci* like members of this biofilm produce hydrogen peroxide that can freely permeate the cell envelopes of neighboring bacteria[64]. Oxidative stress also originates from host defense systems like neutrophils. In short, oxidative stress is ubiquitous in the oral cavity. Hence, survival in the presence of oxygen is critical for the virulence and pathogenicity of *P. gingivalis*[62].

Oxygen may induce a very complex effect on an obligatory anaerobe like *P. gingivalis*. Metabolic products of oxygen like superoxide, hydrogen peroxide and hydroxyl radicals generally create a high redox environment which might lead to oxidation and inactivation of bacterial enzymes. Inactivation of these enzymes is one of the primary reasons for inability of anaerobes to survive in the presence of oxygen. Despite the survival challenges posed by oxygen, *P. gingivalis* possesses a robust defense system that makes it aerotolerent[63].

Genomic sequence of the W83 strain of *P. gingivalis* shows the presence of *oxyR* gene, a homologue of the putative transcriptional regulator associated with oxidative stress[63]. A past study has shown that *P. gingivalis* OxyR shares only 30% identity with that of *E. coli*[63]. Assays done with *P. gingivalis* W83 strain in which *oxyR* is inactivated has shown that this strain grows normally under anaerobic conditions. Sensitivity of *P. gingivalis oxyR* mutant towards oxygen emphasizes the role of *P. gingivalis oxyR* gene in bacterial aerotolerence[62,{Ohara, 2006 #9}].

In *E. coli* and other facultative aerobes and anaerobes, there exists a separate regulator, SoxR, for aerotolerence and the regulator OxyR is utilized only for resistance to hydrogen peroxide[63]. The presence of separate regulators is necessary due to complex respiratory requirements of those bacteria. In an obligate anaerobe like *P. gingivalis,* the *soxRS* regulon is absent which entails the two functions, aerotolerence and resistance to hydrogen peroxide to be combined in a single protein. Phenotypic characterization of the *P. gingivalis oxyR* mutant strain proved that the regulator OxyR is critical for resistance to hydrogen peroxide as well as for aerotolerance[63].

As discussed in the earlier sections, due to increased concentration of intracellular hydrogen peroxide, *E. coli* OxyR rapidly activates the transcription of *OxyS* (a small, non-translated regulatory RNA), *katG* (hydrogen peroxidase I), *gorA* (glutathione reductase), *grxA*

(glutaredoxin), *ahpC* (alkyl hydroperoxidase C) and *dps* (non-specific DNA binding protein). Amongst these, the gene encoding glutaredoxin (*grxA*) and encoding catalase (*katG*) is absent in *PG* genome[63,65]. In *PG*, the genes *ahpFC* and *dps are* regulated by OxyR but they remain uninduced by hydrogen peroxide treatment[63], instead, their expression increases as a result of exposure to atmospheric oxygen[62]. Other than genes mentioned for *E. coli* OxyR, the *PG oxyR* regulon also includes PG0421 (encoding a hypothetical protein with no apparent homology to other oxidative-stress-related genes), *sod* (encoding superoxide dismutase which plays a clear role in protection against oxidative stress), *ftn* (encodes ferritin, an iron storage protein) and *tpx* (encodes a thiol peroxidase)[62,66]. A past study has shown that atmospheric oxygen acts as an inducer for these genes, whereas, hydrogen peroxide is not responsible for elevated expression of these genes[62]. The above observation indicates that in *P. gingivalis,* the stimulus used to induce oxidative stress plays a critical role in transcriptional activation of the *oxyR* regulon.

There are very contradictory views about the expression of *oxyR* regulon in *P. gingivalis*. One view is that in *P. gingivalis*, expression of *oxyR* regulon occurs during anaerobic growth and is independent of intracellular hydrogen peroxide concentration, suggesting that *P. gingivalis* OxyR does not act as sensor of hydrogen peroxide. Even then the expression of this regulon seems to be critical for bacterial resistance to hydrogen peroxide as well as bacterial aerotolerence. This constitutive expression of antioxidant genes might be of an advantage for *P. gingivalis* as oxidative stress is ubiquitous in the oral cavity[63]. Researches are being carried out to investigate the reason behind this constitutive activation of *P. gingivalis* OxyR. A probable reason could be the lack of an effective reducing system to maintain OxyR in its reduced form. In *E .coli*, proteins such as glutaredoxin 1 (*grxA*) and thioredoxin (*trxA*) reduce OxyR[60], among which glutaredoxin is the more effective one. *PG* genome has a homologue of thioredoxin (*trxA*)

which shows 50 % similarity to that of the *E. coli* analog but homologue of glutaredoxin (*grxA*) is absent[63]. Another probable reason suggested by investigators is a possibility that *P. gingivalis* possesses OxyR that is locked in the oxidized conformation due to some structural aspects[63]. The above observations suggest that the regulation of genes by *P. gingivalis* OxyR is different than that occurring in *E. coli* in aspects like the number and types of genes regulated, stimulus for the oxidative stress and conditions under which OxyR remains activated.

Other investigations demonstrated that in *P. gingivalis* expression of *sod* and *ahpC* which was regulated by OxyR was induced by oxidative stress[66]. It was also observed that the expression of *ahpC-F*, *dps*, *ftn*, *tpx* was OxyR-dependent and increased after atmospheric oxygen exposure[62]. These studies support the other view that the expression of *oxyR* regulon is not constitutive, but this regulon is induced under conditions of oxidative stress only. Hence regulation by *P. gingivalis* OxyR is not well understood and needs further investigation.

1.1.7. Preliminary data. To study gene regulation by *P. gingivalis* OxyR microarrays were carried out in lab. Wild type *P. gingivalis* strain and *oxyR* ko strain were used to analyze gene expression. These strains were grown with and without iron (Fe^{2+}) in the growth medium. Wild type *P. gingivalis* strain grown in the media containing iron showed some hints of gene regulation which was not exhibited by the *oxyR* ko strain grown under identical conditions. Interestingly, the same regulation was not exhibited by the wild type strain when it was grown in a media without iron. These results indicate that apart from OxyR, iron also plays a role gene regulation and that OxyR requires iron for regulation of its target genes.

This co-regulation is true vice versa also. For example, the *hmu* operon in *P. gingivalis* is made up of six genes *hmuY, hmuR, hmuS, hmuT, hmuU, hmuV.* All of these encode proteins involved in bacterial hemin uptake. If the surrounding media is rich in hemin, then this operon is

down-regulated, whereas, in iron deplete conditions, this operon is up-regulated[39,67]. Wild type *P. gingivalis* grown under both hemin replete and deplete conditions showed down and up regulation of the operon, respectively. It was observed that this regulation was absent in an *oxyR* mutant *P. gingivalis* strain. The mutant strain was grown in both hemin replete and deplete conditions where it was observed that the *hmu* operon was up-regulated under both the conditions, indicating that the regulation was lost. The above observations indicate that iron also requires OxyR for regulation of its target genes.

These previous studies indicate that some genes are co-regulated by iron and OxyR in *P. gingivalis* suggesting that metals like iron might play a role in OxyR-DNA binding. These predictions form the basis of our hypothesis.

1.1.8. Role of Iron. In the case of *P. gingivalis*, iron is a main nutrient for this periopathogen[39] and plays a pivotal role in its virulence. Studies have demonstrated that when grown under hemin limitation, *P. gingivalis* were less virulent than their counterparts that were grown in excess hemin[68-70]. Although *P. gingivalis* can reside at different locations in the oral cavity, bleeding periodontal pocket is the most favorite niche for this bacterium, the reason behind this can be abundance of iron. Periodontal pockets are bathed in gingival crevicular fluid. Hemoglobin present in this fluid, derived from lysed erythrocytes serve as a main source of hemin for bacterial uptake[39]. These pockets are less exposed to atmospheric oxygen compared to other sites in the oral cavity. Hence, iron is also available for bacterial uptake in ferrous form which is more soluble than its ferric analog.

Intracellular iron concentration has a connection with oxidative stress experienced by the bacteria. Iron has a tendency of getting oxidized and reduced readily. This capability of iron makes it biochemically dangerous, because free iron in the form of ferrous ion is capable of

undergoing *Fenton reaction* which converts hydrogen peroxide into harmful free radicals[39]. Though iron and hemin are critical for growth and virulence of *P. gingivalis*, keeping a check on the intracellular free iron concentration is also important.

In micro-organisms, 10-20% of all genes are regulated by intracellular iron concentration and *P. gingivalis* is not an exception. An alteration in the expression of 71 genes was observed when grown in iron limited conditions, many of which were related to iron uptake-storage, adhesion with the host cells, biofilm formation and many were genes of unknown function[39]. The genes which were down-regulated in iron limited conditions included genes encoding proteins implicated in iron storage and those involved in oxidative stress defense. Some of the genes like a gene encoding Dps (ferritin like protein), gene encoding Ftn (ferritin), gene encoding rubrerythrin, were of special interest as they also come under *oxyR* regulon. Dps comes under OxyR regulon and is proved to be required for protection against oxidative stress[71]. The protein rubrerythrin is predicted to be indispensable for the protection of *P. gingivalis* from oxidative stress[72]. Genes induced by oxidative stress are down-regulated in iron deplete conditions[39] indicating a connection between oxidative stress, OxyR and iron.

1.1.9. Present research. Based on the preliminary studies, the goal of this present study is to determine the binding mechanism of OxyR to DNA and to establish the hypothesis that metals are involved in OxyR-DNA binding. This research encompasses the following investigations:

1. Determination of the DNA sequence binding site for OxyR
2. Establishing the role of metals in OxyR-DNA binding
3. Role of specific amino acids in DNA binding
4. *In-vivo* characterization of OxyR-DNA binding

1.1.10. Principle and significance of in vivo characterization. Recently, *in vivo* kinetics behind specific binding of a transcription factor, *lac* repressor (LacI) to a chromosomal *lac* operator was studied by Elf et al.[73] For imaging purposes, *lac* repressor was tagged with a rapidly maturing fluorescent protein (YFP) at its C-terminus. The fusion protein was expressed from the native chromosomal *lacI* locus. C-terminal fusion is preferred over N-terminal fusion to avoid interference with N-terminal DNA-binding domain. To detect association-dissociation of LacI with its target binding site, *lac* operator on the *E. coli* genome, *E. coli* cells were imaged with a wide field fluorescence microscope and a charged-coupled device (CCD) camera in presence and absence of IPTG. The presence of IPTG substantially reduces the affinity of LacI to *lac* operator resulting in dissociation of LacI from *lac* operator.[74] It was observed that in the presence of IPTG, when the LacI was not bound to the *lac* operator, a diffuse fluorescent signal was detected from the entire area of the cell. In absence of IPTG, when LacI was bound to *lac* operator sharp fluorescent spots were observed.

These studies established the basic concept that if a fluorescently tagged transcription factor is not specifically bound to DNA, it emits fluorescence from the entire area of the cell due to its fast diffusion. When the transcription factor is bound specifically to relatively stationary DNA fragment, it emits from a highly localized region.[75] This phenomenon is referred as *fluorescence due to localization enhancement*.

Based on this concept, fluorescently tagged OxyR will produce sharp fluorescent spots when bound to target DNA sequences whereas, a diffused signal will be obtained for unbound OxyR. This phenomenon allows investigation of the conditions under which *P. gingivalis* OxyR binds to its target DNA sequences present on *P. gingivalis* genomic DNA, by direct visualization of binding. By keeping this idea in mind the ultimate goal of in vivo characterization is to

investigate *P. gingivalis* OxyR-DNA binding by growing the cells under different conditions like in the presence and absence of metals and EDTA in the growth media. These experiments would allow us to validate the results obtained through in vitro characterization and to confirm the role of metals in OxyR-DNA binding. By using this technique, it is also possible to compare if the fluorescently tagged *P. gingivalis* OxyR and fluorescently tagged *E. coli* OxyR bind to their respective target sequences under similar conditions. Direct visualization of in vivo binding is the best technique to study binding mechanism of a transcription factor to its target sequences, since it nullifies the need of extrapolating the results obtained by in vitro experiments where the experimental conditions may not be the replica of intracellular atmosphere.

1.2 Materials and methods.

1.2.1. Constructs used. Construct **A** was made in the lab by cloning sequence encoding *P. gingivalis* OxyR from *P. gingivalis* genomic DNA in to pFC20K T7 SP6 Halo Tag Flexi Vector (Promega) in place of *barnase* gene. Protocol given in the technical manual of Flexi vector system was followed for cloning. An erythromycin resistant cassette, *ermF-ermAM* (Fletcher) was inserted downstream of HaloTag sequence at EcoRI/XbaI. A sequence encoding *ssb* gene from *P. gingivalis* genomic DNA was inserted downstream of the ermF-ermAM at XbaI/SalI. A site directed mutagenesis was performed on plasmid DNA from construct **A** to prepare construct **B** and **C**. A QuickChange Lightening Site-Directed Mutagenesis kit (Agilent technologies) was used. Construct **D** was prepared by cloning sequence encoding OxyR from *E. coli* genomic DNA in to pFC20K T7 SP6 Halo Tag Flexi Vector (Promega) in place of *barnase* gene.

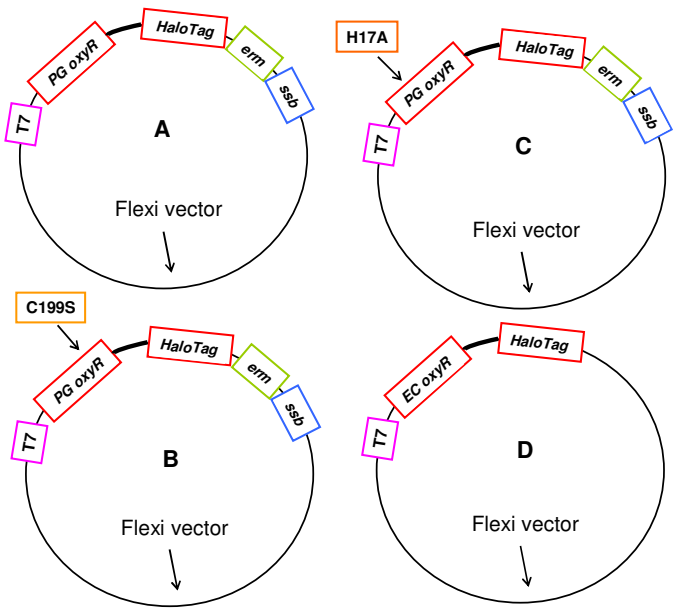

Constructs used for protein expression

1.2.2. Protein expression and purification. To express wild type *P. gingivalis* OxyR, mutant OxyR-C199S, mutant OxyR-H17A and wild type *E. coli* OxyR along with a Halo tag at the C-terminus, constructs **A**, **B**, **C**, **D** were used respectively. These constructs were transformed in *E.*

coli BL21(DE3) expression cells and the transformed strains were named as V3080, V3082, V3099 and V3107 respectively. These strains were used for protein purification. The cultures for all the strains were treated in a similar manner as mentioned ahead. A 50 ml LB media containing 25 µg/ml Kanamycin and 100 mg of glucose was inoculated with the transformants growing on a fresh LB-Kanamycin plate. This media was left in the shaker at 37°C for 12-16 hours. This 50 ml media was used to inoculate 500 ml LB media containing 25 µg/ml Kanamycin and 1 gm of glucose. Media was left in the shaker at 37°C till the optical density reaches 0.6. 1 mM isopropyl-β-D-thiogalactopyranoside (IPTG) was added to induce the protein expression. The media was left in the shaker at 37°C overnight after addition of IPTG. For harvesting the pellet and further purification, Halo Tag protein purification system protocol (Promega) was followed.

1.2.3. Running a protein gel. The purified protein samples were run on a NuPage12% Bis-Tris gel (Invitrogen). Samples were run under two conditions, non-reducing and reducing. Under non-reducing conditions, protein samples were mixed with NuPage LDS sample buffer (4X) and loaded on the gel. Under reducing conditions, NuPage LDS sample buffer (4X), Invitrogen-reducing agent (10X) were added in the protein sample of interest, heated on near boiling water bath for 10 minutes before loading on the gel. Gels were run at 200V.

1.2.4. Preparation of cell lysates. For preparation of cell lysates for *P. gingivalis* wild type OxyR, *P. gingivalis* mutant OxyR-C199S and *P. gingivalis* mutant OxyR-H17A, strains V3080, V3082 and V3099 are utilized respectively. A 5 ml LB media, containing 25 µg/ml Kanamycin was inoculated with the desired strain. The culture was left in the shaker at 37°C till the optical density reaches 0.6. Half of the culture was stored on ice till isolation of the pellet. This pellet was used to prepare the un-induced cell- lysate. The remaining half of the culture at optical

density 0.6 was induced by addition of 1 mM IPTG and left in the shaker at 37°C for four hours. Pellet was harvested. This pellet was used to prepare induced-cell lysate. Pellets for un-induced and induced lysates were washed twice with 1X PBS. The cultures were placed in Lysing matrix tubes (MP Biomedicals). For breaking the cells Fastprep-24 (MP Biomedicals) was used twice for 30 second at the speed of 6. Samples were spun down at 13,000 RPM, 4°C for 5 minutes in a table top centrifuge. Supernatants were directly used for EMSA.

***1.2.5. Preparation and purification of in vitro protein*.** TNT Quick Coupled Transcription/Translation System protocol was followed for *in vitro* protein production. This process requires a plasmid DNA in which sequence encoding the protein of interest is cloned downstream T7 promoter. For *P. gingivalis* wild type OxyR, plasmid DNA isolated from strain V3080 was used. Similarly for mutant proteins C199S and H17A, plasmid DNA isolated from strains V3082 and V3099 were utilized respectively.

The entire 50 µl transcription-translation reaction was treated as 10 ml cell culture and Halo Tag Protein Purification system protocol was followed with some modifications. For example, after incubation with TEV protease, supernatant was not applied to the His-link resin obtained with the kit. Instead, the 5 mM zinc was added to the supernatant to inactivate TEV protease. This supernatant is used to set binding reaction of EMSA.

1.2.6. Labeling the DNA probes for EMSA. DNA probes that are to be used for EMSA were amplified by PCR from *P. gingivalis* W83 genomic DNA and *E. coli BL21(DE3)* genomic DNA as per the requirement. Refer to list of primers 1 for primer sequences and size of the fragments amplified. PCR amplified probes were purified using PCR purification kit (Quiagen). Biotin 3' End DNA Labeling Kit (Thermo-Scientific) was utilized to label the probes. Approximately a little less than 5000 nM of the purified fragments were used for one labeling reaction (50 µl).

Volume of the labeled DNA used for binding with the protein was different in each assay as mentioned in result section.

1.2.7. Binding conditions used for EMSA. EMSAs were carried out under two different binding conditions. Under condition A, the components added were 2 µl of 10X binding buffer, 1 µl of poly (dI.dC), 1 µl of 50% glycerol, 1 µl of 1% NP-40, 1 µl of 1M KCl, 1 µl of 100mM MgCl2, 1 µl of 200 mM EDTA, 1 µl of 1X BSA in a total of 20 µl of binding reaction (These components were provided along with the Chemiluminiscent EMSA binding reaction kit by Promega) . Under condition B, NP-40 and glycerol were excluded and Tween-20 (final concentration = 1%) was added to the binding reaction.

1.2.8. Running gel for EMSA and transfer to the Nylon membrane. For running the binding reaction on a gel, 6% Polyacrylamide as well as Agarose gel is used depending on the size of the probe. Whenever samples were run on a polyacrylamide gel, protocol from the Instructions manual of Lightshift Chemiluminiscent EMSA kit (Thermo Scientific) was followed for gel running and transfer. When agarose gel is used, 1X TBE buffer is used as a running buffer. After electrophoresis, gel is soaked in denaturing buffer for half an hour followed by soaking in neutralizing buffer for an hour. Transfer to Amershan Hybond – N^+ membrane (GE Healthcare) is achieved under gravity by keeping the gel and the membrane in contact with each other for about 10 hours. Denaturing buffer was prepared by adding 8 gm of sodium hydroxide and 35 gm of sodium chloride to water and final volume was adjusted to 400 ml. Neutralization buffer was prepared by adding 30.8 gm of ammonium acetate and 320 mg of sodium chloride to water and final volume was adjusted to 400ml.

1.2.9. Detection by chemiluminiscence. Once the transfer is accomplished, the membrane is UV crosslinked (Stratagene 2400) and DNA signal is detected by chemiluminiscence using Lightshift Chemiluminiscent detection module (Thermo Scientific).

1.2.10. CHIP-chip assay. To determine the target binding sites present on *P. gingivalis* genomic DNA for *P. gingivalis* OxyR, CHIP-chip assay was performed in the lab by Sai Yanamandra. For that, construct **A** mentioned in section *1.2.1* was utilized. This construct was electroporated in *P. gingivalis W83* after linearization. Incorporation of C-terminally tagged *P. gingivalis* OxyR into *P. gingivalis* genomic DNA by homologous recombination, was confirmed by genomic DNA sequencing. This recombination led to the expression of *P. gingivalis* OxyR along with a HaloTag from genomic DNA and its subsequent binding to the target sites present on the genomic DNA. OxyR bound to the target sites on the genome was cross-linked. A resin that binds covalently with the tag was used to pool this cross-linked OxyR. Protocol for the Halo-CHIP system (Promega) was followed to pool OxyR and to purify the bound genomic DNA fragments after releasing the cross-links. The purified fragments were utilized for whole genome amplification and library generation. Microarrays were performed which provided a list of fragments (Refer table 1) bound to the transcriptional regulator OxyR.

1.2.11. Construction and working of a microfluidic flow plate for bacteria (ONIX-CeLLASIC system). Microfluidic plates are suitable for bacterial live cell microscopy. B04A plate fits to a typical microscope stage holder. The microfluidic chambers on the

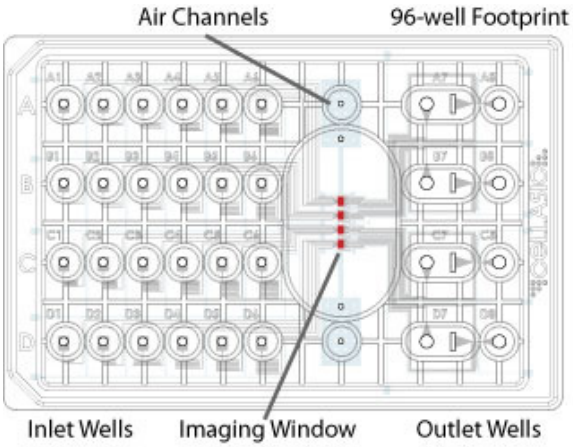

A

plates hold the bacterial cells in a single focal plane and they can be tracked over multiple generations for >12 hours. The design of the plate is as shown in the diagram ***A*** (Images **A**, **B** and **C**: courtesy www.cellasic.com). Rows A-D on the plate are 4 independent flow units. Each unit has 8 wells including 5 inlets for adding media (1-5), cell outlet (6), waste (7) and cell inlet (8) from which culture can be introduced in the plate. Each independent flow unit has 6 trap regions (1-6) each having different dimensions as shown in diagram ***B***. The cell-loading in these trap regions is a two step process. In the first step, flow from well 8 to 6 transports the cell culture loaded in cell-inlet well 8 into the bottom flow channel. The next step is to pressurize both well 6 and 8 to drive cells into the 6 trap regions. The cells will get trapped in the trap channels depending on their size. For application of this pressure the lid of the plate is connected to a CeLLASIC unit as shown in the diagram ***C***. Precision laminar flow creates a stable cell environment resulting in minimal stress on cells. B04A plate allows 5 different solution changes during one experiment as there are 5 inlet wells

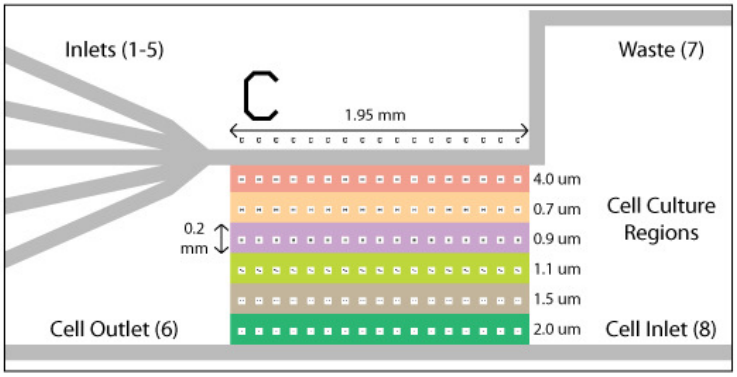

B

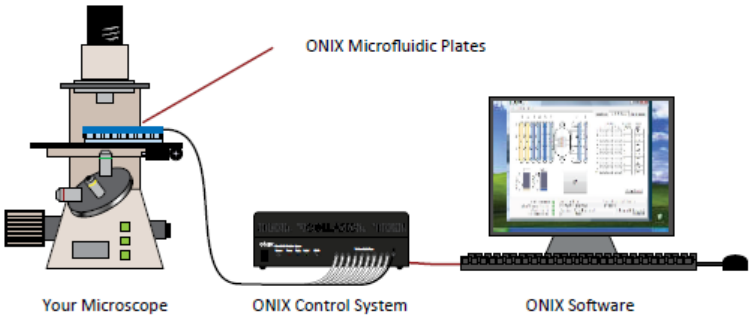

C

for the media in one flow channel. CellASIC FG Software allows programming automated perfusion protocols for precise change in the media at the desired time point. It is possible to record cell response to media change during high magnification imaging.

***1.2.12. Culture preparation for approach* 1.** A 5 ml LB media containing 25 µg/ml Kanamycin was inoculated with strain V3080 from a freshly streaked plate. Culture was allowed to grow at 37°C for 18 hours. After the incubation period, the culture was diluted by a factor of 10. 50 µl of the diluted cell culture was put in well 8 of the independent flow channel A of the microfluidic plate. The composition of the media added in all the inlet channels 1-5 was not same. In well 1 and well 2, 300 µl of LB media was added. In wells 3-5, 300 µl of LB media containing 1X Halo Tag ligand and 1mM IPTG was added. The dilutions of the HaloTag ligand were made as per the technical manual of HaloTag Technology: *Focus On Imaging* (Promega). The media in which the cells were bathing was changed after each hour such that the cells were bathing in the media from inlet 1 for first one hour, then in the media from inlet 2 for the next one hour and so on. All the instrumental set up was made as mentioned in the B04A Application Note for *Dynamic Live Cell Imaging For Bacteria* (CeLLASIC). Images were captured using *Zeiss Cell Observer Spinning Disc Microscope* after every 15 minutes for 5 hours.

1.2.13. Design of strategy 1 for approach 2. pGLOW-Bs2-Stop(pUC18) vector bought from 'evocatal' had the fluorescent protein in a pUC18 vector which was unsuitable for expression. To construct and express a fusion protein it was necessary to clone pGLOW-Bs2 from pUC18 downstream and in frame with *P. gingivalis* OxyR already present in Flexi vector (plasmid DNA V3080). In this plasmid V3080 'HaloTag coding sequence' was present downstream *P. gingivalis* OxyR. Our cloning strategy was based on replacement of the HaloTag coding sequence with the sequence encoding pGLOW-Bs2. To achieve this aim, plasmid DNA V3080

should be digested with restriction enzymes Xhoi, EcoRi which will digest out the HaloTag protein coding sequence. pGLOW-Bs2 coding sequence then can be inserted in between these restriction sites in frame with the OxyR present upstream. For this purpose a new construct was made from original pGLOW-Bs2-Stop (pUC18) bought from the company in the lab. This new construct was made by inserting some new sequences and deleting some existing sequences from the original pUC18 vector that contained pGLOW-Bs2-Stop as explained ahead. T7 promoter sequence, multiple cloning sites, and the sequence encoding TEV protease all taken from pFC20K HaloTag T7 SP6 Flexi vector were cloned upstream the start codon for pGLOW-Bs2 in pUC18 vector. This resulted in insertion of Xhoi recognition site upstream pGLOW-Bs2 start codon in the pUC18 vector. At the end of the coding sequence for Bs2 there was a Xhoi recognition sequence CTC GAG encoding Leucine and Glutamic acid. Presence of this sequence was undesirable for our cloning strategy. Hence this sequence was deleted keeping the Stop codon downstream intact. EcoRi recognition sequence was inserted downstream the stop codon.

1.2.14. Xhoi/EcoRi double digestion. Plasmid DNAs or amplified PCR products were digested using Xhoi, EcoRi, NEB 10X buffer 2, 100X BSA and water. Concentrations of the DNA to be digested and the restriction enzymes used, was adjusted according to the NEB guidelines for digestion. The digestion reactions are incubated at 37°C for 2 hours and then run on agarose gel of desired concentration according to the size of the DNA fragment digested.

1.2.15. Gel extraction, ligation, transformation. A Quiagen gel extraction kit was used to excise and extract the desired bands from the gel. Flexi ligation kit (Promega) was used and ligation protocol from the technical manual for Flexi vector systems (Promega) was followed. Ligation reactions were transformed in *E. coli* XL-10 ultracompetent cells following the protocol provided by Invitrogen.

1.2.16. Culture preparation for the construct made by strategy 1. To check the expression by fluorescence, the newly ligated construct mentioned in section *1.4.2.I.* was transformed into *E. coli BL21(DE3)* expression cells (Invitrogen). The transformed cells were used to inoculate 5 ml LB media containing 25 µg/ml of kanamycin. The culture was left in the shaker at 37°C for 18 hours. After dilution by a factor of 10 the culture was allowed to grow till the O.D. reaches 0.6 and then induced by adding 1mM IPTG. Culture was again left in the shaker at 37°C for 4 hours after induction. 10 µl of this culture were directly put on a microscope slide and a cover-slip was put. The culture was observed under a fluorescent microscope once the culture was dry.

1.2.17. Design of constructs for strategy 2 approach 2. Under strategy 2, three constructs were made. For making these constructs, it was planned to make use of the plasmid DNA isolated from strain V3107 (which expresses *E. coli* OxyR tagged to a HaloTag protein) and the plasmid DNA isolated from the strain V3080 (which expresses *P. gingivalis* OxyR tagged to a HaloTag protein) Construct ***P*** was designed as shown in the adjacent diagram. *AGGAGA* is the RBS for *E. coli*. It was planned to make construct ***P*** by replacing HaloTag in V3107 plasmid. Similarly by replacing HaloTag in V3080 plasmid DNA construct ***Q*** could be made. Constructs ***P*** and ***Q*** could be transformed in *E. coli BL21(DE3)* cells to monitor expression of *E. coli* OxyR and *P. gingivalis* OxyR respectively in *E. coli* cells and to visualize their binding to *E. coli* genomic DNA under different conditions for comparison of the binding mechanisms. Design for construct ***R*** was similar to that of construct ***Q*** except that in place of *E. coli* RBS, *P. gingivalis* RBS was planned to be inserted to allow the expression of the fusion protein and visualization of its binding inside *P. gingivalis* cells.

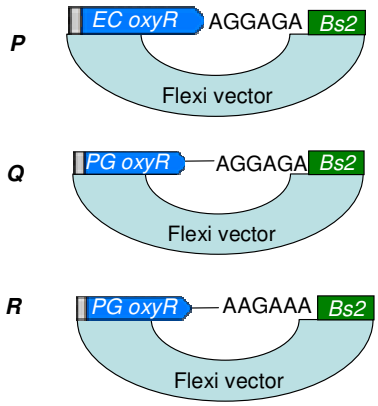

1.2.18. Amplification of inserts for strategy 2. For amplification of inserts for strategy 2, plasmid pGLOW-Bs2-Stop (pUC18) (evoglow) was used as a template for PCR. To amplify inserts to clone in constructs ***P and Q*** the sequence of the forward primer (FP1) used was -

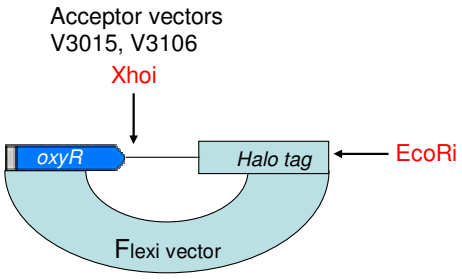

GAGCTCTCGAGTGAGGAGATATGGCGTCGTTCCAGTCGTTCGGCATCCCG. This primer inserted the Xhoi site and the sequence encoding *E. coli* RBS upstream of the start codon of pGLOW-Bs2. The primer sequence was designed in such a way that pGLOW-Bs2 will be in frame with OxyR after cloning. The sequence of the reverse primer (RP) used for insertion in these constructs was – CTGACTGAATTCTCATTCAAGCAGCTTTTCATATTCCTTCTG. This reverse primer was designed to insert EcoRi recognition sequence downstream the stop codon of pGLOW-Bs2. In the sequence encoding Bs2, the last two codons are CTC GAG encoding amino acids Leucine and Glutamic acid respectively. As CTC GAG is recognition sequence for Xhoi, these codons were changed to CTT GAA again encoding amino acids Leucine and Glutamic acid, respectively. This resulted in the elimination of Xhoi recognition sequence present at the end of bs2 encoding sequence as it was unsuitable for the planned cloning strategy. For insertion into construct ***R,*** sequence of the forward primer (FP2) used was GAGCTCTCGAGAAATAAGAAACAATTATGGCGTCGTTCCAG. This was designed to insert Xhoi site and *P. gingivalis* RBS upstream the start codon of Bs2. Primer design was to keep Bs2 in frame with OxyR. A total of three inserts, two amplified with primer pair FP1-RP and one amplified with primer pair FP2-RP were run on the gel to check the size of the PCR product. Inserts amplified with FP1-RP were used for ligating with vectors V3107 and V3080

after digestion to make constructs ***P*** and ***Q***, respectively. Insert amplified with FP2-RP was ligated with Vector V3080 post digestion to make construct ***R***.

1.2.19. TOPO cloning. Insetrs were amplified with primer pairs FP1-RP and FP2-RP using pGLOW-Bs2-Stop(pUC18) (evoglow) as template. These PCR products were purified using Quiagen PCR purification kit and cloned into TOPO2.1 PCR vector (Invitrogen) by following the ligation protocol provided in the technical manual for TOPO vectors (Invitrogen).

1.2.20. Construction of a positive control vector. The sequence encoding pGLOW-Bs2 was cloned downstream the T7 promoter in the present in Flexi vector replacing the *barnase* gene. pFC20K halo Tag T7 SP6 Flexi vector was available from promega as shown in G.

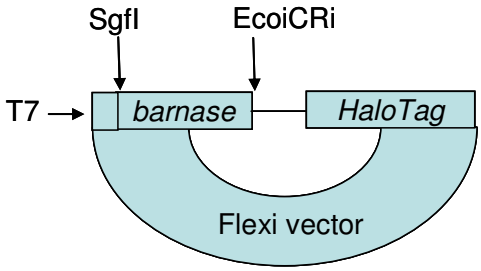

G

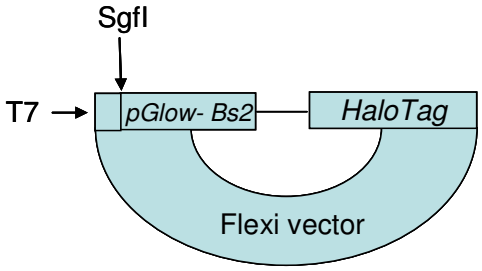

E

The aimed positive control construct is as shown in E. pGLOW-Bs2 coding sequence was amplified from pGLOW-Bs2-stop(pUC18) vector from evocatal basic kit with forward primer having sgfI site and reverse primer having pmeI site. Sequence of the forward primer used was 5'-ATATGCGATCGCCATGGCGTCGTTCCAGTCGTTC-3' and sequence of the reverse primer used was 5'- GGTTGTTTAAACTCACTCGAGCAGCTTTTCATATTCCT. Purified and amplified PCR product and the Flexi vector were digested and ligated by following the protocol

mentioned in the 'Technical manual of Flexi Vector Systems.' After colony screening, plasmid DNA was isolated and sent for sequencing.

1.2.21. Culture treatment for controls. The positive control construct was transformed into *E. coli BL21(DE3)* expression cells (Invitrogen). A 5 ml LB media containing 25 µg/ml Kanamycin was inoculated with those transformed cells and left in the shaker at 37°C for 18 hours. The culture was diluted by a factor of 10 and again left in shaker at 37°C till O.D. reaches 0.5-0.7. The culture was divided in three parts and 0.2 mM, 0.4mM and1 mM IPTG was added in them to induce protein expression. All the three induced cultures were left in the shaker at 25°C for 18 hours. The culture was spun at 6000 RPM for 5 minutes at 4°C. The pellet was re-suspended in 1 ml of 1X PBS buffer and 10 µl of that was put on microscope slide and a cover-slip was put. The slide was observed under the fluorescent microscope once the culture dried. A culture for strain V3080 was also grown and induced under the same conditions as mentioned above for the positive control construct and used as a negative control.

1.2.22. Camera settings. Nurolucida camera settings used were, for DIC 55 ms, gain 2, for CFP and DAPI 1200 ms, gain 6, for GFP and DsRed 700 ms, gain 4. In all cases offset was 4.

1.3 Results of *in vitro* characterization

1.3.1 Selection of DNA fragments to check OxyR binding. *In vitro* characterization of binding of *P. gingivalis* OxyR to genomic DNA, starts with the prediction of sites present on the *P. gingivalis* genomic DNA which act as target binding sites for *P. gingivalis* OxyR. For this prediction, a CHIP-chip assay was carried out in the lab by Sai Yanamandra as mentioned in the materials and methods section. This assay provided a list DNA fragments which were found to be the target binding sites for *P. gingivalis* OxyR (Refer to table 1). These fragments were amplified from the *P. gingivalis* genomic DNA by PCR (Refer to list of primers 1 for primer sequences), purified and labeled as mentioned in the materials and methods section for their use in electrophoretic mobility shift assays (EMSA). Microarray studies mentioned in preliminary studies section indicated that *rbr* and *hmu* fragments are also the target binding sites for *P. gingivalis* OxyR. Along with these fragments a few more fragments reported to bind with *P. gingivalis* OxyR in literature are used for EMSAs. They include *sod*[62,66] (encoding superoxide dismutase), *ahpc*[62] (encoding alkyl hydroperoxidase C). Three different regions from *sod* fragment and two different regions from the *ahpc* fragments were amplified with respective primers for their use in EMSA. Fragment *is* is the predicted binding site for *E. coli* OxyR[61], hence it is also used whenever *E. coli* OxyR was used for EMSA. (Primer sequences for all the DNA fragments are as mentioned in list of primers 1).

1.3.2 Optimizing conditions for EMSA EMSAs were performed to validate the results obtained by CHIP-chip assay. Conditions under which EMSAs can be performed include several variables like design of the nucleic acid target, purification of protein to be used for binding, binding reaction components, incubation span and temperature for the binding reaction and

Table 1. List of DNA fragments from CHIP-chip assay.

Gene bank locus tag	Definition
PG0360	LemA protein (conserved hypothetical protein)
PG1863	Hypothetical protein
PG1862	Hypothetical protein
PG0304	Electron transport complex
PG1240	conserved hypothetical protein (probable transcription regulator)
PG1307	glucose inhibited division protein B (glucose-inhibited division protein B)
PG0964	(CDP-diacylglycerol-serine-O-phosphatidyltransferase)

electrophoresis conditions. These variables need to be optimized for each molecular system[76].

***1.3.2.I. EMSA control* reaction under two different binding conditions.** As mentioned in the materials and methods section, two different conditions A and B were utilized to set binding reactions. Condition B differs from condition A as B does not contain glycerol and NP-40, instead Tween 20 was added in the binding reaction. Role of glycerol is to stabilize labile proteins and also to enhance the stability of protein-DNA complexes. Non-ionic detergents such as NP-40 and Tween 20 help to maximize protein solubility[76]. It was observed in the lab earlier that replacement of glycerol and NP-40 by Tween-20, increased the clarity and sharpness of the signal obtained. On the other hand, under this condition B, total absence of glycerol in the binding reaction might decrease the stability of DNA-protein complex to give false negative results. Hence it was decided to try EMSAs under both the binding conditions. For that, EMSA was carried out on the as received control samples under both the conditions. Control reactions were carried out as per the protocol given in the instructions manual of Lightshift Chemiluminiscent EMSA kit (Thermo Scientific). Binding reactions were run on 6% polyacrylamide native gel (Invitrogen). Transfer and detection were performed as mentioned in the materials and methods section.

Lane 1 in figure 1A and B, containing only labeled DNA marks the position of unbound DNA fragment on the gel. Second lane shows a band of less mobility indicating the formation of DNA-protein complex. This band of less mobility disappears in the third lane indicating that protein does not bind to the labeled DNA fragment when excess of unlabeled specific competitor was added to the binding reaction prior to the addition of the labeled fragment. Figure 1 shows that control reaction carried out using commercially available products worked as expected under

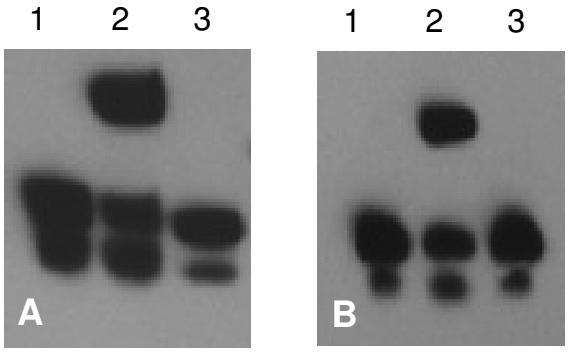

Figure 1. EMSA of the as received protein and DNA fragment performed under two different conditions, A and B, as mentioned in the text. Lane 1 – Biotin-EBNA control DNA, Lane 2 - Biotin-EBNA control DNA+ EBNA extract, Lane 3 - Biotin EBNA control DNA+ EBNA extract+ 200-molar excess of unlabeled EBNA DNA.

both the binding reaction conditions. The next step was to try EMSAs using the protein of interest and its target DNA fragments.

1.3.2.II Making different protein preparations for EMSA.

1.3.2.II A. In vivo protein expression and Purification. Wild type *P. gingivalis* OxyR and OxyR mutants C199S and H17A were expressed in *E. coli* cells and purified simultaneously as mentioned in the materials and methods section. The final yields for purified wild type protein preparations, mutant C199S and mutant H17A were 0.9mg/ml, 0.55 mg/ml and 0.04 mg/ml respectively. A 12% Bis-tris gel was run to check the purity of the protein preps. (Figure 2). 15µl of each of the preparations were loaded on the denaturing gel under non-reducing conditions. (Refer to materials and methods section for details on sample preparation.)

In figure 2, Lane 4 in panels A, B and C contains the purified protein. A single band of 50 kDa was observed for all the three purified protein preparations indicating that the preparations did not contain any other proteins than the one of interest. Although the size of Size of *P. gingivalis* OxyR is 35 kDa and that of *E. coli* OxyR is 33 kDa, of the band observed for all the three protein preparations was of 50 kDa size. This could be due to intra-molecular disulfide bond formation.

1.3.2.II.B. Preparation of crude protein lysates. Instead of purified proteins, crude cell lysates were used for binding with the DNA fragments of interest. Un-induced and induced cell lysates were prepared for wild type *P. gingivalis* OxyR as well as for mutant OxyR proteins C199S and H17A as mentioned in the materials and methods section. Lysates for wild type protein and lysates for mutant proteins were not prepared simultaneously.

1.3.2.II.C. Preparation of in vitro transcribed OxyR. Wild type *P. gingivalis* OxyR and OxyR mutant proteins C199S and H17A were made *in vitro* by using *in vitro* transcription-translation

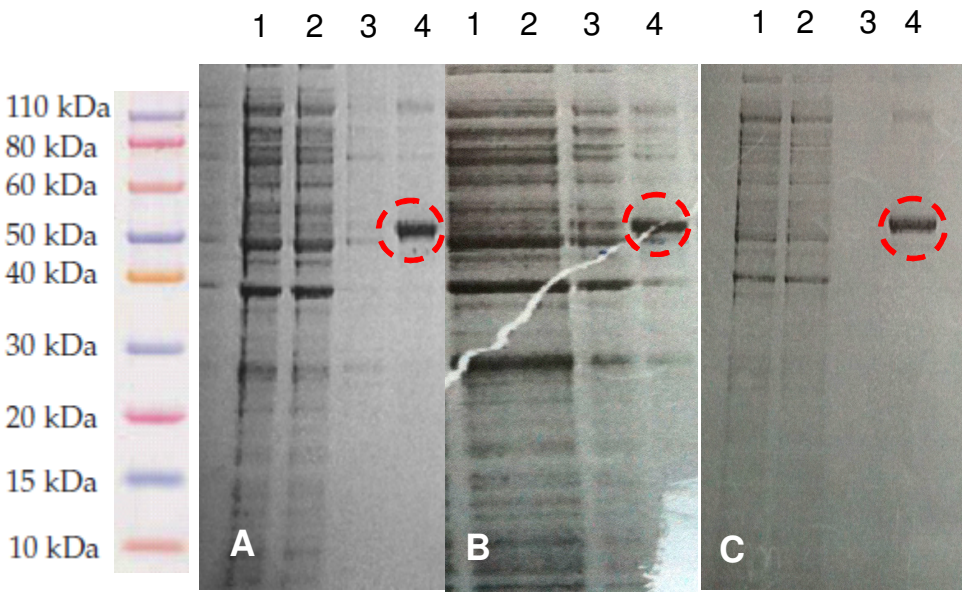

Figure 2. SDS-PAGE gel image for the *in vivo* expressed and purified *P. gingivalis* OxyR wild type (A), OxyR mutant C199S (B), OxyR mutant H17A (C); where Lane L – Novex sharp pre-stained ladder (Invitrogen), Lane 1 – Cell lysate, Lane 2 – Flow through, Lane 3 – Resin wash, Lane 4- Elution 1.

kit and purified as mentioned in the materials and methods section. To check the size and purity of the *in vitro* transcribed protein, 30 µl of the wild type *in vitro* OxyR preparations made in the subsequent batches were run on 12% Bis-tris denaturing gel under non-reducing conditions. (Figure 3) A band of 50 KD was observed for *in vitro* wild type OxyR preparations from batch 2, 3 and 4. An undesired band of 15 kDa was also observed for all the three preparations.

1.3.3. Binding of OxyR to selected fragments.

1.3.3.I. EMSAs using purified proteins. Wild type OxyR and mutant proteins C199S and H17A purified after in vivo expression (Refer section *1.3.2.II.A*) were used to bind with *rbr* fragment amplified from *P. gingivalis* genomic DNA (Primers sequences are mentioned in the list of primers 1) after purification and labeling of the fragment as mentioned in materials and methods section. 5 µl of the labeled DNA fragment was utilized for binding with 1 µg of each of the above mentioned protein preparations under two different binding conditions A and B mentioned in materials and methods section. The binding reactions were run on a 3% Agarose gel. Figure 4 shows that all the DNA fragments, those which were not incubated with the protein and those which were incubated with protein had the same mobility indicating that none of the proteins incubated with labeled *rbr* fragment were able to bind to the fragment.

Wild type purified OxyR was used to perform EMSAs with different DNA fragments amplified from *P. gingivalis* genomic DNA, which were the predicted binding sites for wild type OxyR. Three different parts of the *sod* gene were used for EMSAs (Refer section *1.3.1* for details)(Figure not included). CHIP-chip assay listed genes PG0964 and PG0360 as probable binding sites. So these were also used for EMSAs (Figure not included).None of these binding reactions showed a shift in the position of the DNA fragment after incubating predicted OxyR

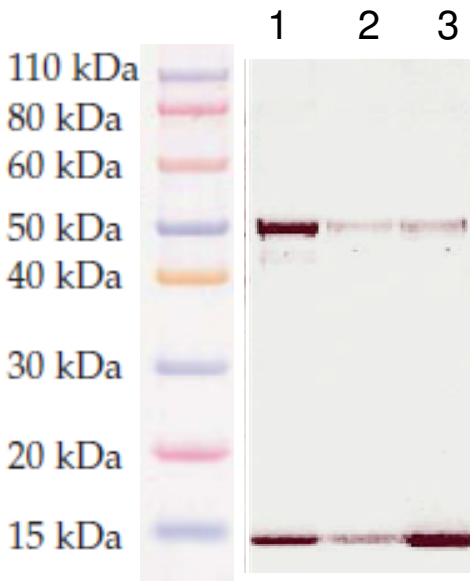

Figure 3. SDS-PAGE gel image of the *in vitro* transcribed *P. gingivalis* OxyR from different batches, where Lane 1 – Novex sharp pre-stained ledder (Invitrogen), Lane 2-4 – *In vitro* transcribed wild type P. gingivalis OxyR from batches 2, 3 and 4 respectively.

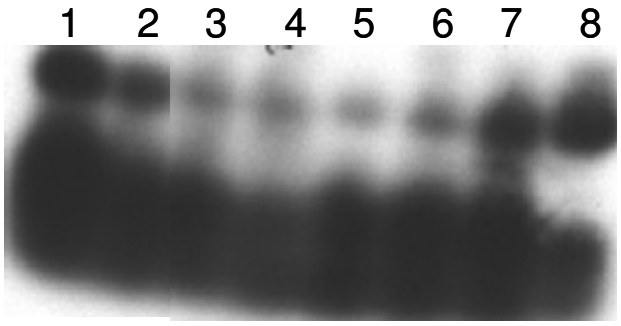

Figure 4. EMSA using (*rbr*) DNA fragment with the purified proteins, where lanes 1-4 - condition A and lanes 5-8 - repetition of lanes 1-4 under condition B. Lane 1 - *rbr* DNA only, Lane 2 – *rbr* DNA+ Wt. OxyR, Lane 3 - *rbr* DNA+ OxyR mutant C199S, Lane 4 - *rb*r DNA+ OxyR mutant H17A

binding DNA fragments with the wild type *P. gingivalis* OxyR protein suggesting that purified *P. gingivalis* OxyR does not bind to the predicted DNA sites.

***1.3.3.II. EMSAs using crude protein extract for wild type* OxyR .** Different amounts of crude protein extracts prepared for wild type OxyR were used to perform EMSAs. First, 3 µl of lysates were used to bind with 5 µl of labeled DNA fragments *sod* part 3 and PG1240 IFF,IFR (For primer sequences, refer to the list of primers 1) (Figure 5). 5.5 µl of lysates were used to bind with 5 µl of labeled fragments PG0964, PG0304 and PG1307 (For primer sequences refer to the list primers 1) (Figure 6). All these EMSAs were carried out under condition B mentioned in materials and methods section. The binding reactions were run on a 1% Agarose gel.

In figure 5 and 6, lane 1 marks the position of the unbound DNA. In lane 2, un-induced lysates served as negative controls as there is no change in the mobility of the DNA fragments after incubation with the un-induced lysates. Lane 3 indicates that the mobility of the fragments used, decreased after incubation with the induced lysates suggesting formation of a protein-DNA complex with all the DNA fragments used.

1.3.3.III. EMSA using in vitro wild type OxyR. 3.12 µg of the wild type OxyR protein purified after producing it *in vitro,* was used for binding with 5 µl of labeled DNA fragments. DNA fragments PG0964, PG1307, PG0304, PG1240 F,R, PG1240 IFF, IFR, PG1862 IFF, IFR and PG0360 were used (Refer to table 1 and the list of primers 1 for details). EMSAs were carried out under condition B. The binding reactions were run on a 1% Agarose gel.

Figure 7 shows the image of the EMSA using different DNA fragments. For each fragment the first lane marks the position of the unbound DNA fragment. For all the DNA fragments shown in figure 7, the mobility decreased after incubation of the respective fragments with the wild type protein indicating the formation of a protein-DNA complex in each case.

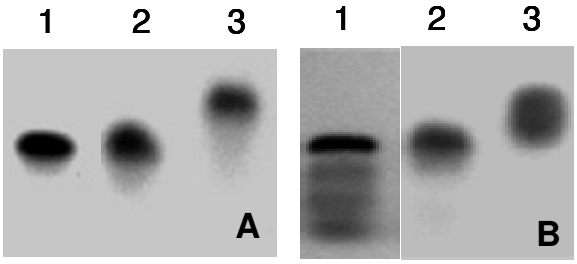

Figure 5. EMSA using wild type OxyR cell lysates (volume – 3 µl) with DNA fragments PG1240 (A) and *sod* 3(B), where, Lane 1 – DNA only, Lane 2 – DNA+ un-induced OxyR cell lysate, Lane 3 – DNA+ Induced OxyR cell lysate.

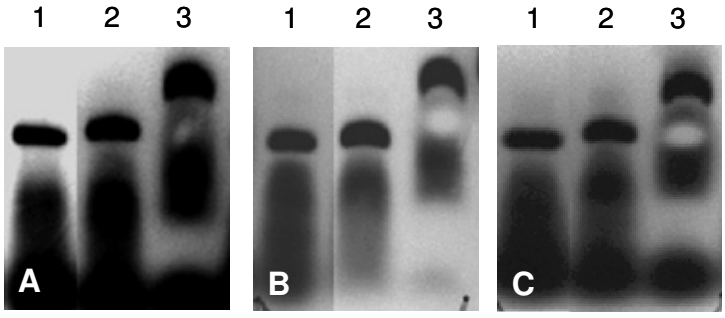

Figure 6. EMSA using wild type OxyR cell lysates (volume – 5.5 µl) with DNA fragment PG0964 (A), PG0304 (B) and PG1307 (C) where, Lane 1 – DNA only, Lane 2 – DNA+ un-induced OxyR cell lysate, Lane 3 – DNA+ Induced OxyR cell lysate.

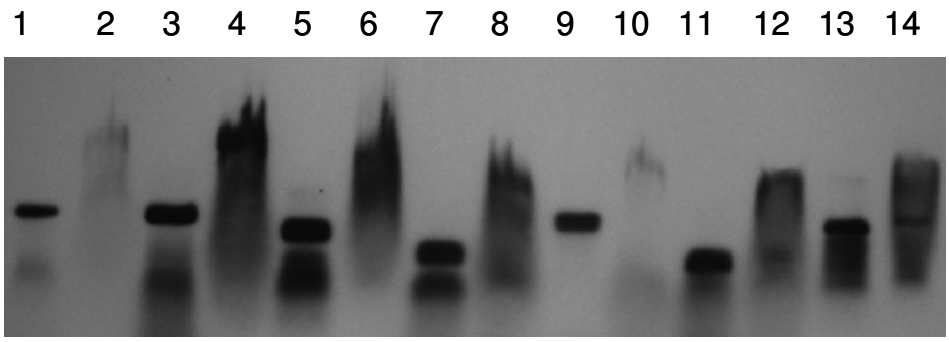

Figure 7. EMSA using In vitro transcribed wild type OxyR with different DNA fragments, where, Lane 1 - DNA only (PG0964), Lane 2 - DNA + OxyR, Lane 3 - DNA only (PG1307), Lane 4 - DNA + OxyR, Lane 5 - DNA only (PG0304), Lane 6 - DNA + OxyR, Lane 7 - DNA only (PG 1240 F,R), Lane 8 - DNA + OxyR, Lane 9 - DNA only (PG 1240 IFR, IRR), Lane 10 - DNA + OxyR, Lane 11 - DNA only (PG1862), Lane 12 - DNA + OxyR, Lane 13 - DNA only (PG0360), Lane 14 - DNA + OxyR.

Decrease in mobility was apparent in the form of smears but no distinct band of less mobility was observed for any of the fragments. This may be due to partial dissociation of the protein-DNA complex during electrophoresis.

1.3.4 EMSAs to investigate the effect of increase in the amount of protein and the effect of EDTA treatment. EMSA was performed using different concentrations of the *in vitro* wild type *P. gingivalis* OxyR in the binding reaction. The amount of protein in each binding reaction was increased keeping the amount of the labeled DNA used for binding, the same. 5 µl of the labeled DNA fragments PG0964 (Figure 8A) and *hmu* (Figure 8B) were used for each binding reaction (Refer to table 1 and the list of primers 1 for details). EMSAs were carried under condition B.

Lane 1 marks the position of unbound DNA on the gel. Lanes 2,3,5,6 contain binding reactions set with increasing concentrations of OxyR. For PG0964 it was evident that with 1 µg and 1.87 µg of protein a partial shift was observed. With 2.5 µg and 3.12 µg of protein smears were observed. For *hmu,* 1 µg and 1.87 µg of protein was not capable to decrease the mobility of the DNA fragment clearly. But smears were observed when protein concentration above 2.5 µg was used for binding indicating the formation of protein-DNA complex in these cases.

To check if the metal chelator EDTA has any effect on OxyR-DNA binding, protein was treated with 0.33M EDTA for half an hour before using it for binding with the DNA fragment. Lane 4 in figure 8A and 8B has the binding reaction carried out in the presence of EDTA-treated protein. Although the amount of protein in lane 4 is same as that in lane 3, lane 4 does not show the partial shift which was evident in lane 3. This indicated that the metal chelator EDTA might be responsible for abrogating the shift.

To further investigate the effect of EDTA on OxyR-DNA binding, EMSA was again carried out using 5 µl of labeled DNA fragments PG0964, *hmu*. Part 2 and 3 of the *sod* fragment

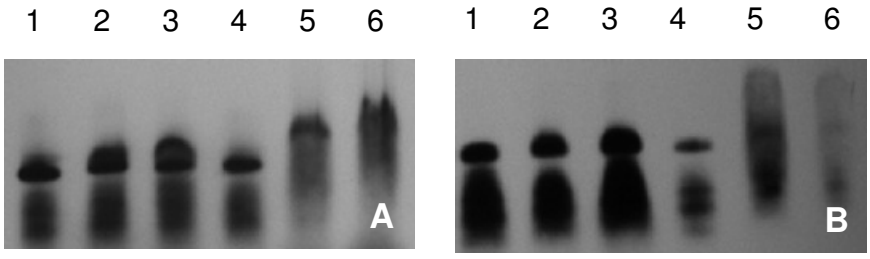

Figure 8. EMSA using different concentrations of *in vitro* transcribed wild type OxyR
with DNA fragment PG0964 (A) and *hmu* (B), where Lane 1 – DNA only, Lane 2 - DNA+ 1 µg OxyR, Lane 3 - DNA+ 1.87 µg OxyR, Lane 4 - DNA+ 1.87 µg OxyR treated with 0.33M EDTA, Lane 5 - DNA+ 2.5 µg OxyR, Lane 6- DNA+ 3.12 µg OxyR.

were also used. This time more protein was utilized for binding than used in Figure 8 and the concentration of EDTA used for treating the protein was lesser (Refer figure 9 for details). Protein was treated with EDTA for half an hour before setting the binding reaction. EMSAs were carried out under condition B. Un-treated 2.73 µg of OxyR binds to the DNA fragments used, evident by the smear in lane 2, indicating that there is a decrease in the mobility of the DNA fragment after incubating it with the untreated wild type OxyR. Lane 3 has the binding reaction in which treated OxyR was utilized. No smear or shift in the position of DNA is evident in this lane indicating that OxyR has not bound to the DNA fragment.

1.3.5. EMSA using mutant proteins.

1.3.5.I.. EMSA using crude lysates of the mutant proteins. Crude lysates were prepared for mutant OxyR proteins, C199S and H17A as mentioned in section *1.3.2.II.B*. 5.5 µl of these lysates were used to set binding reactions with 5 µl of the labeled DNA fragments PG0964. PG0304, PG1307 (Figure 10). (Refer to list of primers for primer sequences.) Again, in these images the first lane marks the position of the unbound DNA fragment. The un-induced lysates serve as negative controls. DNA fragments did not show clear shift after incubation with induced lysates of the mutant proteins.

One drawback of the EMSAs shown in figure 10A was, accidentally, less than 1mM IPTG was used for protein expression while making the induced cell lysates. To prepare the mutant cell lysates exactly in the same manner as prepared for wild type lysates, fresh cell lysates were prepared for mutant C199S using 1mM IPTG for induction. EMSA was repeated using this new cell lysate (Figure 10B). Any shift in the position of DNA fragments was not evident with the new lysates of the mutant protein as well. All EMSAs using lysates were carried out under condition B.

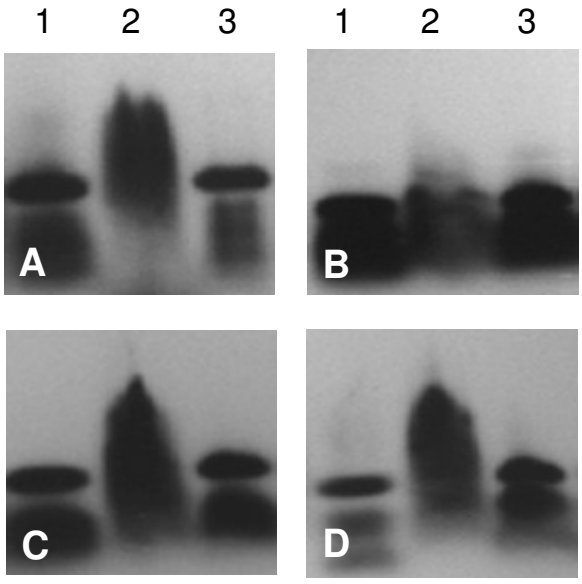

Figure 9. EMSA for verification of effect of EDTA on binding of *in vitro* transcribed wild type OxyR using DNA fragment PG0964 (A), *hmu* (B), *sod*-2 (C) and *sod*-3 (D), where Lane 1 – DNA only, Lane 2 - DNA+ 2.73 µg OxyR, Lane 3 - DNA+ 2.73 µg OxyR treated with 0.13M EDTA.

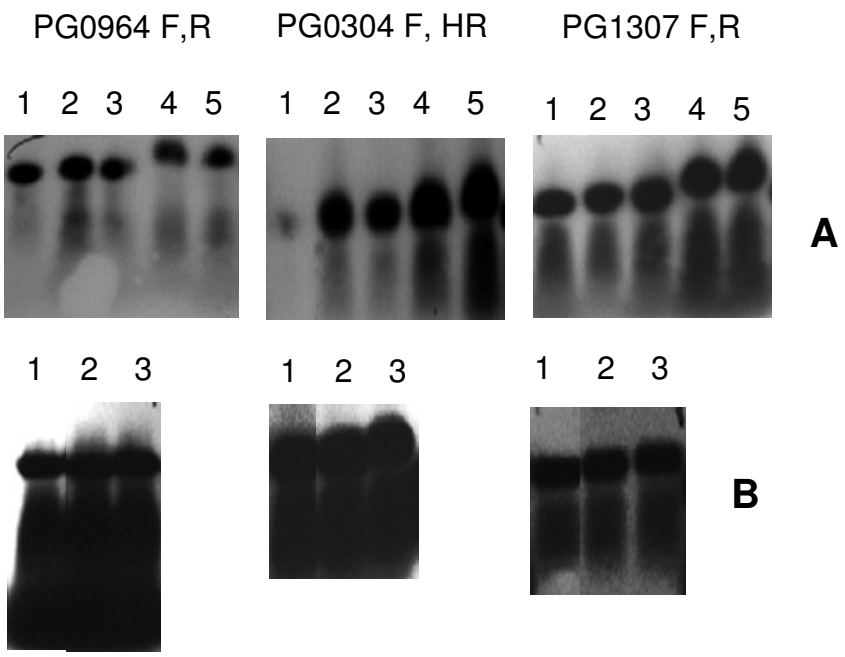

Figure 10. EMSA using mutant OxyR cell lysates, where, A – IPTG < 1 mM and B – IPTG = 1 mM. Lane 1 – DNA only, Lane 2 – DNA+ un-induced mutant C199S cell lysate, Lane 3 – DNA+ Induced mutant C199S cell lysate, Lane 4 – DNA+ un-induced mutant H17A cell lysate, Lane 5 – DNA+ Induced mutant H17A cell lysate.

1.3.5.II. EMSA using in vitro mutant proteins. As *in vitro* transcribed wild type *P. gingivalis* OxyR was able to bind with the DNA fragments used, we were interested in knowing whether the OxyR muatants C199S and H17A bind to those fragments or not. These mutant proteins were made as mentioned in section *1.3.2.II.C* and as mentioned in the materials and methods section. EMSAs were carried out using 1.7 µg of each of these mutant proteins for binding with 5 µl of the labeled DNA fragments. 1.7 µg of *in vitro* transcribed wild type OxyR was used as a positive control. Fragments used were PG1307 (Figure 11A), *hmu* (Figure 11B) and PG0964 (Figure 11C) (Refer table 1 and the list of primers 1 for details regarding DNA fragments).

Lane 1 marks the position of the unbound DNA. Lane 2 containing binding reaction with the wild type protein shows shift in the position of the DNA fragment indicating the formation of DNA-OxyR complex. Such a shift is not observed in lanes 3 and 4 suggesting that the mutant proteins are not binding with the DNA fragment.

1.3.6. Comparison between P. gingivalis OxyR and E. coli OxyR binding.

1.3.6.I. Protein expression and purification. To compare the binding of *P. gingivalis* OxyR and *E. coli* OxyR to their predicted binding sites, we performed EMSAs with both of them. For that a fresh batch of proteins was prepared. Wild type *P. gingivalis* OxyR and wild type *E. coli* OxyR were expressed in *E.coli BL21(DE3)* cells and purified using Halo resin replicating the protocol used in section *1.3.2.II.A* and in materials and methods section. A denaturing gel is run by loading 5 µg of the purified proteins under reducing and non-reducing conditions to check the purity of the sample (Figure 12). For *P. gingivalis* OxyR and for *E. coli* OxyR a prominent band at 37 KD was observed under reducing and non-reducing conditions.

1.3.6.II. EMSAs using freshly purified E. coli OxyR and P. gingivalis OxyR. EMSAs were performed using freshly purified *E. coli* OxyR and *P. gingivalis* OxyR. The protein

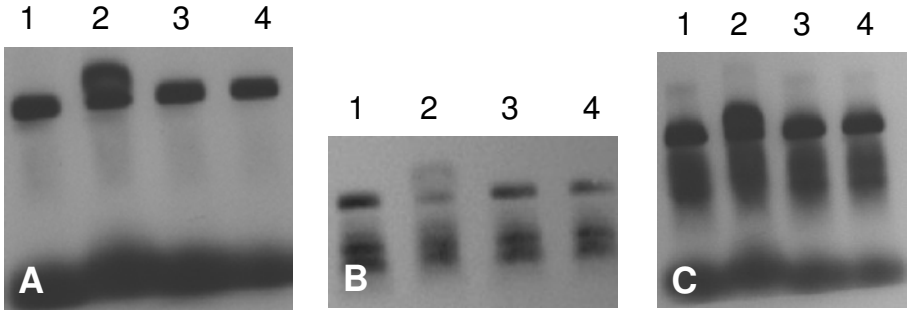

Figure 11. EMSA using *in vitro* transcribed OxyR mutants with DNA fragments PG1307 (A), *hmu* (B) and PG0964 (C) where Lane 1- DNA only, Lane 2 - DNA+ Wt. OxyR, Lane 3- DNA+ mutant C199S, Lane 4- DNA+ mutant H123A.

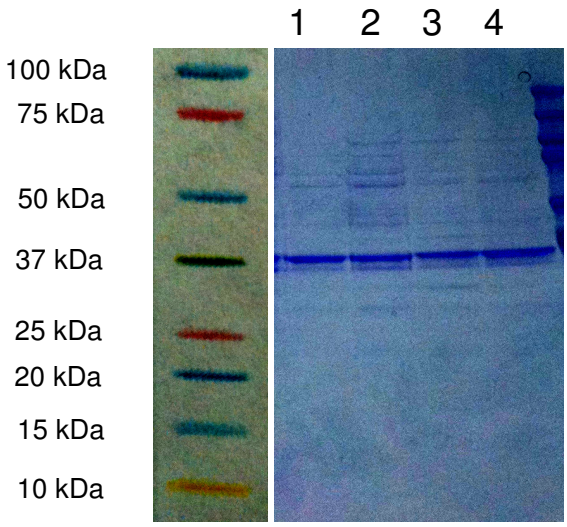

Figure 12. SDS-PAGE gel image of the purified *P. gingivalis* OxyR and *E. coli* OxyR from batch 2, where Lane 1 – *P. gingivalis* OxyR under non-reducing conditions, Lane 2 – *E. coli* OxyR under non-reducing conditions, Lane 3 – *P. gingivalis* OxyR under reducing conditions, Lane 4 – *E. coli* OxyR under reducing conditions.

concentrations were immeasurably low. So 10.5 µl of each of the proteins were used to set each binding reaction without concentrating the proteins. 1.5 µl of the labeled DNA fragment was used to set each binding reaction. As the aim was to compare binding by *E. coli* OxyR and *P. gingivalis* OxyR, DNA fragments utilized for EMSAs were among the predicted binding sites for either *P. gingivalis* OxyR or *E. coli* OxyR. Fragments used were *IS* , PGahpc1, PGahpc2, *hmu* (Refer to section *1.3.1* and list of primers 1 for details on DNA fragments used) (Figure 13A). A 3% agarose gel was used for running the binding reactions. Fragments used earlier with in vitro *P. gingivalis* OxyR were also used for example, PG0964 and PG0360 (Figure 13B). A 1% agarose gel was used to run the binding reactions (Refer table 1 and the list of primers 1 for details regarding the DNA fragments). The components added in the binding reaction for this EMSA were same as those mentioned for condition A in materials and methods section except the amount of glycerol added was increased to 5% and EDTA was excluded from the binding reaction. Running buffer and gel buffer were prepared as mentioned in the materials and methods section with 5% glycerol added in both of them. A higher amount of glycerol was used for these assays as glycerol enhances the stability of the protein-DNA complex(48). Assays mentioned in section *1.3.2.VI* , indicated the role of EDTA in abrogating binding, hence EDTA was excluded from the binding reaction.

IGS protein (4 µg treated with hemin and DTT) and IGS DNA fragments were used just as experimental positive controls. IGS protein when treated with hemin under reducing conditions, binds to its target DNA site, serving as positive control (Figure 13A, lanes 1, 2). Though not complete, IS fragment showed a clear shift when incubated with *E. coli* OxyR. There was no change in the mobility of IS fragment when incubated with P. gingivalis OxyR (Figure 13A, lanes 3-5). PGahpc1 and PGahpc2 showed a partial shift on incubation with *E. coli* OxyR

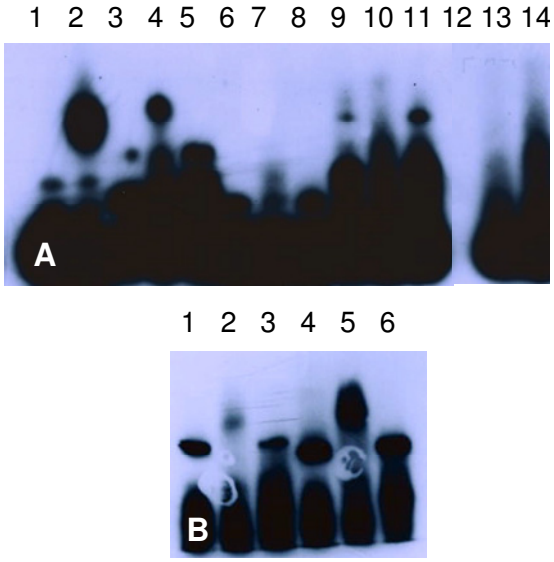

Figure 13. EMSA using fresh purified wild type *P. gingivalis* OxyR and *E. coli* OxyR with different DNA fragments. A. Lane 1 – IGS DNA only, Lane 2 – IGS DNA + IGS protein treated with hemin, Lane 3 – IS DNA only, Lane 4 – IS DNA + *E. coli* OxyR, Lane 5 – IS DNA + *P. gingivalis* OxyR, Lane 6 – PG ahpc1 DNA only, Lane 7 - PG ahpc1 DNA + *E. coli* OxyR, Lane 8 - PG ahpc1 DNA + *P. gingivalis* OxyR, Lane 9 – PG ahpc2 DNA only, Lane 10 – PG ahpc2 DNA + *E. coli* OxyR, Lane 11 - PG ahpc2 DNA + *P. gingivalis* OxyR, Lane 12 – *hmu* DNA only, Lane 13 – *hmu* DNA + *E. coli* OxyR Lane 14 - *hmu* DNA + *P. gingivalis* OxyR
B. Lane 1 – PG0964 DNA only, Lane 2 - PG0964 DNA + *E. coli* OxyR, Lane 3 - PG0964 DNA + *P. gingivalis* OxyR, Lane 4 – PG0360 DNA only + Lane 5 – PG0360 DNA + *E. coli* OxyR, Lane 6 - PG0360 DNA + *P. gingivalis* OxyR.

but not with *P. gingivalis* OxyR (Figure 13A, lanes 6-11). EMSAs done using *hmu* fragment were not conclusive (Figure 13A, lanes 12-14). For DNA fragments PG0964 and PG0360, incubation with *E. coli* OxyR resulted in a complete shift in the position of the DNA fragment indicating that *E. coli* OxyR binds to those fragments. But no shift was observed when these fragments were incubated *P. gingivalis* OxyR indicating that purified *P. gingivalis* OxyR does not bind to those fragments. These results were consistent with those mentioned in section 1.3.3. , where EMSAs were performed using purified, *P. gingivalis* OxyR.

For this EMSA, as the concentrations of both the proteins used were not same, it was not appropriate to conclude anything. There was a possibility that concentration of *P. gingivalis* OxyR was so low that there was no visible change in the mobility of the fragment incubated with the protein. One more EMSA was performed exactly in the same manner, where equal concentrations of the two proteins were used to set the binding reactions. Proteins were concentrated using Centrifugal filter units (Millipore). 3.12 µg of each of the proteins was used with 1.5 µl of the labeled DNA fragment in a binding reaction.

IGS protein was again used along with IGS fragment. Untreated IGS protein which does not bind to its target site, served as an experimental negative control. IGS protein treated with hemin under reducing conditions, served as experimental positive control (Figure 14A, lanes 1-3). When incubated with *E. coli* OxyR, IS DNA fragment shows some smear suggesting that there is decrease in the mobility of the fragment due to formation of a DNA-protein complex. But this is not very well clear from the gel picture (Figure 14A, lanes 4-6). Thickness of the DNA-band for PGahpc1 fragment decreased after incubation with *E. coli* OxyR as compared to that for only DNA and after incubation with *P. gingivalis* OxyR (Figure 14A, lanes 7-9). Binding reactions with fragments, PGahpc2 and *hmu* did not show a clear shift Figure 14A, lanes 10-15).

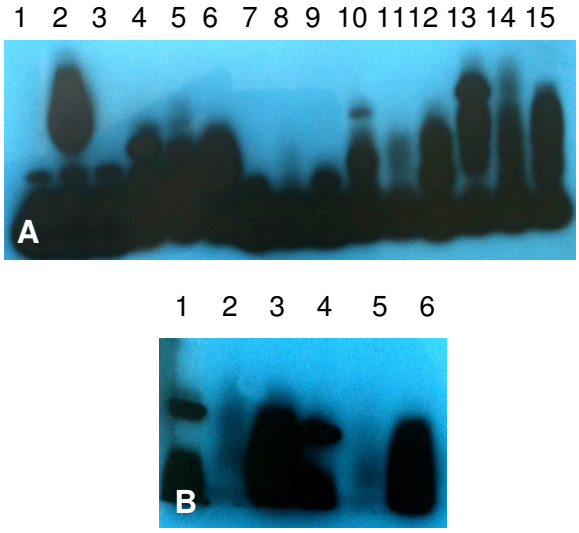

Figure 14. EMSA using equal concentrations of purified wild type *P. gingivalis* OxyR and *E. coli* OxyR with different DNA fragments. A. Lane 1 – IGS DNA only, Lane 2 – IGS DNA + IGS protein treated with hemin, Lane 3 - IGS DNA + IGS untreated protein, Lane 4 – IS DNA only, Lane 5 – IS DNA + *E. coli* OxyR, Lane 6 – IS DNA + *P. gingivalis* OxyR, Lane 7 – PG ahpc1 DNA only, Lane 8 - PG ahpc1 DNA + *E. coli* OxyR, Lane 9 - PG ahpc1 DNA + *P. gingivalis* OxyR, Lane 10 – PG ahpc2 DNA only, Lane 11 – PG ahpc2 DNA + *E. coli* OxyR, Lane 12 - PG ahpc2 DNA + *P. gingivalis* OxyR, Lane 13 – *hmu* DNA only, Lane 14 – *hmu* DNA + *E. coli* OxyR Lane 15 - *hmu* DNA + *P. gingivalis* OxyR (Refer tables .. and … for details regarding DNA fragments).
B. Lane 1 – PG0964 DNA only, Lane 2 - PG0964 DNA + *E. coli* OxyR, Lane 3 - PG0964 DNA + *P. gingivalis* OxyR, Lane 4 – PG0360 DNA only + Lane 5 – PG0360 DNA + *E. coli* OxyR, Lane 6 - PG0360 DNA + *P. gingivalis* OxyR.

Fragments PG0964 and PG0360 showed a faint smear after incubation with *E. coli* OxyR. The DNA band as observed in lane 1 and 4 of figure14B was lost. This suggests that the fragments might be binding with the protein which decreased their mobility drastically. That was why a clear band was not observed in these lanes. After incubation with *P. gingivalis* OxyR there was no change in the mobility of the fragments indicating that again purified *P. gingivalis* OxyR did not bind to the fragments (Figure 14B, lanes 1-6).

All of the EMSAs mentioned above showed that the *in vivo* expressed and purified *P. gingivalis* OxyR does not bind to the predicted target DNA fragments while *E. coli* OxyR produced and treated in the same manner bind to its own target fragment as well as to the target fragment of *P. gingivalis* OxyR. The crude lysate of wild type *P. gingivalis* OxyR and the *in vitro* wild type *P. gingivalis* OxyR bound to the predicted binding sites but the results were not reproducible.

1.4. Results of in vivo characterization. The aim of *in vivo* characterization was to visualize OxyR-DNA binding under a fluorescent microscope.

1.4.1. Approach 1 The first step towards visualizing direct binding of OxyR to its target DNA sequences was to observe expression of OxyR under fluorescent microscope. Strain V3080 was used for this purpose. Strain V3080 consists of *E. coli BL21(DE3)* expression cells which express *P. gingivalis* OxyR with a Halo tag at its C-terminus, from an expression vector. (For details on the strain and vector refer to materials and methods section *1.2.1*) A Halo Tag TMRDirect ligand (Promega) which consists of a red-fluorescent reporter group and a reactive linker that binds covalently to the Halo tag protein was used to check expression of OxyR under fluorescent microscope with the help of a live cell microscopy experiment as described in materials and methods section *1.2.12.* For this experiment, 'microfluidic flow plate for bacteria' (ONIX- CeLLASIC) was utilized. (Principle and design of the microfluidic plate used for this experiment have been elucidated in materials and methods section *1.2.11*.)

Figure 15 displays the images captured during the experiment. First two inlet wells contained only LB media allowing the cells to grow for the first two hours of the experiment. The cells started to express protein when the media from inlet 3 was introduced as it contained the inducer of protein expression, IPTG. Media from inlet 3 also contained the fluorescent ligand which bound covalently with the HaloTag protein expressed along with OxyR, emitting a red fluorescence confirming the protein expression. With time the number of cells increased which can be seen from DIC images (Figure 15A). The protein expression also increased over time as indicated by increase in fluorescence with time (Figure 15B).

The HaloTag TMRDirect ligand proved to be useful for visualizing the expression of *P. gingivalis* OxyR tagged with a HaloTag protein under fluorescent microscope but some of the

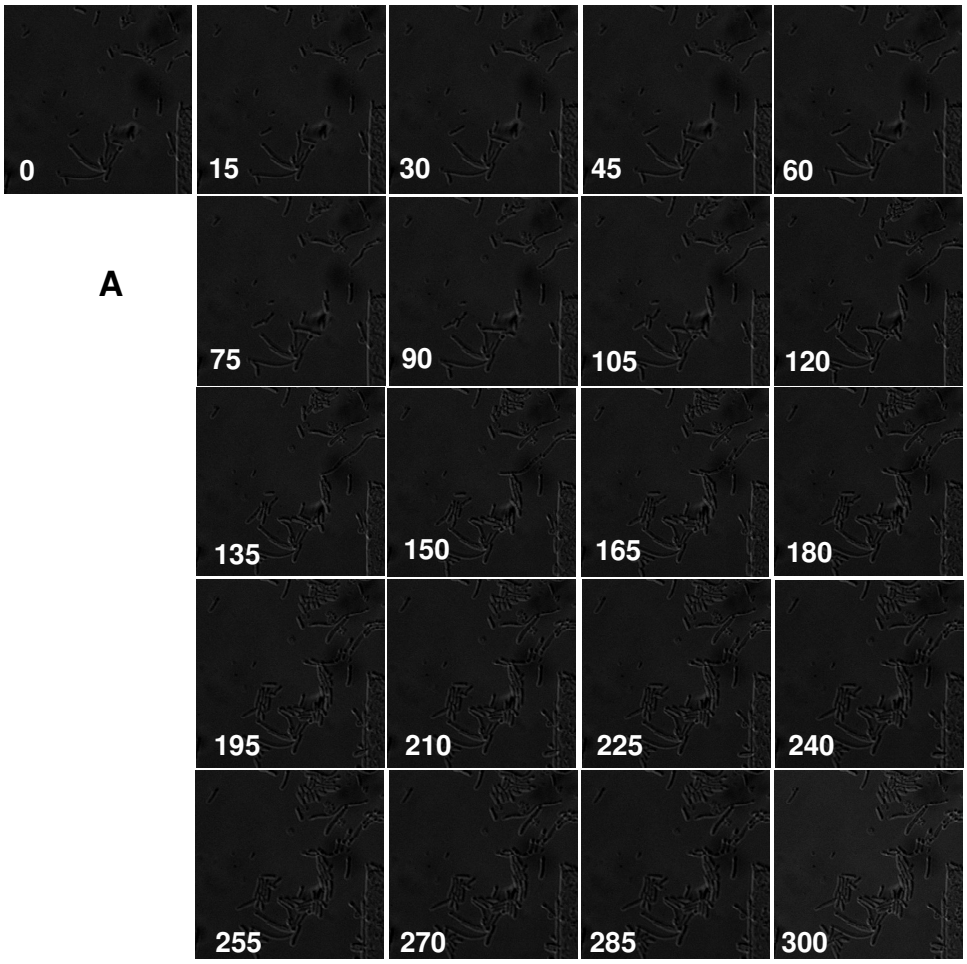

Figure 15A. DIC (Differential interference contrast) images of the live cell microscopy experiment to monitor OxyR expression in real time captured on *Zeiss Cell Observer Spinning Disc Microscope* after every 15 minutes, starting from 0 minute to 5 hours.

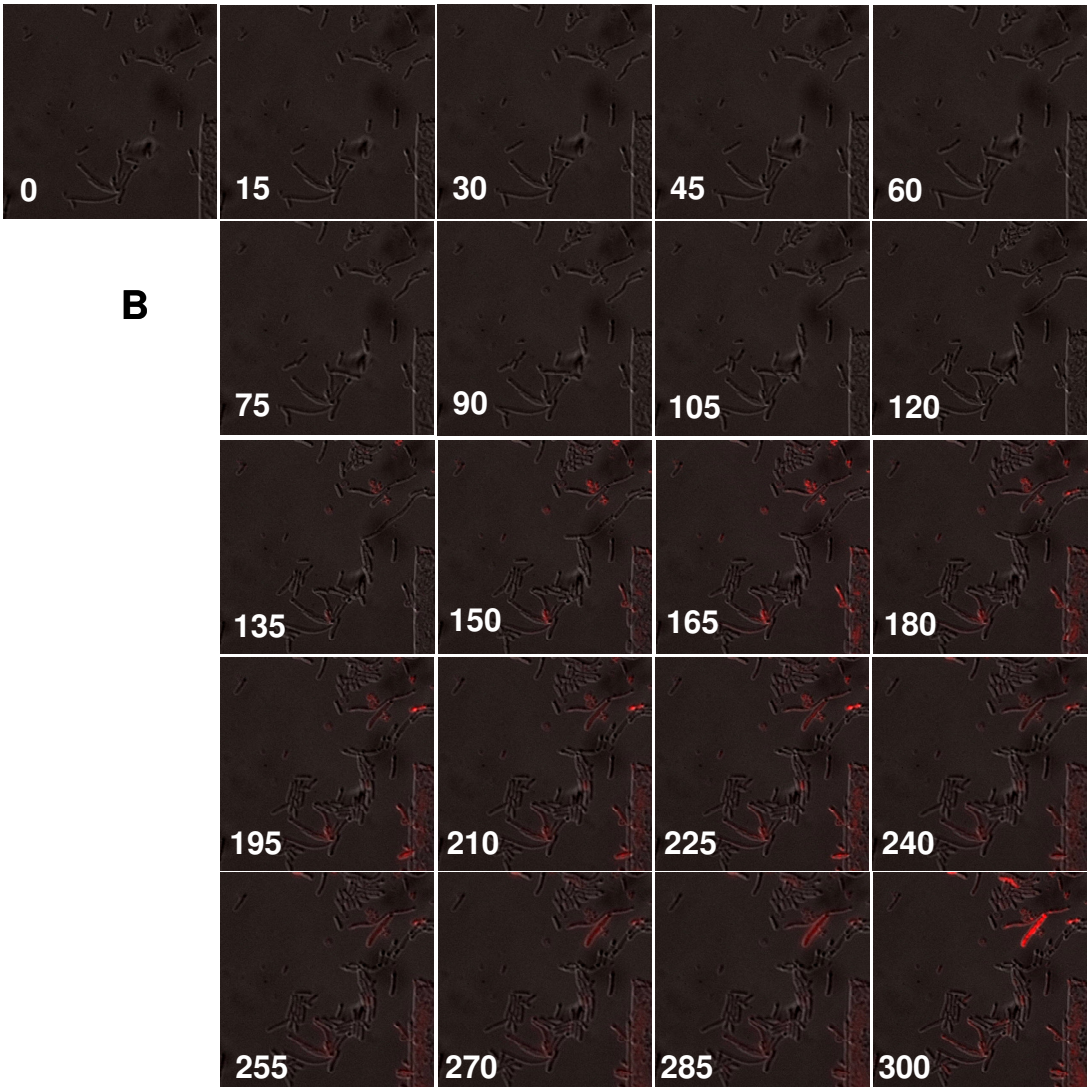

Figure 15 B. Overlay of DIC + fluorescence images from the live cell microscopy experiment to monitor OxyR expression in real time captured on *Zeiss Cell Observer Spinning Disc Microscope* after every 15 minutes, starting from 0 minute to 5 hours.

aspects observed during the experiment made the use of ligand unsuitable for the further investigation. For example, it was observed that the inclusion bodies were catching the ligand earlier than the intracellular Halo-tagged OxyR suggesting that there can be a time-lag between expression of the protein and penetration of ligand in the cells. Another observation that all the cells in the given population were not uniformly emitting the red fluorescence suggested that the dye may not be penetrating all the cells uniformly. To avoid these pitfalls we decided to follow approach 2.

1.4.2. Approach 2 Instead of using some external fluorescent agent like the ligand, expressing OxyR as a fusion protein fused with a fluorescent protein is definitely a better strategy. For this purpose, GFP (green fluorescent protein) and its various sophisticated analogues are the most commonly used fluorescent probes in molecular biology[77]. A major drawback of all the members of the GFP family is that they require molecular oxygen for the synthesis of their respective chromophores, making them unsuitable to use as fluorescent probes under strict anaerobic conditions[78]. As the ultimate goal of our step by step investigation is to observe OxyR-DNA binding *in vivo* in *P. gingivalis* which is an obligate anaerobic bacterium, GFP derivatives are of no use. This fact prompted the use of a flavin mononucleotide (FMN) based fluorescent protein (FbFP) for making a fusion protein with OxyR. The FMN-based protein pGLOW-Bs2 consists of the photoactive domain of the blue-light photoreceptor YtvA derived from *B. subtilis* in which Cys62 is mutagenized to Ala62 to increase the fluorescent intensity[79]. Thus, the aim of approach 2 was to express OxyR as a fusion protein with pGLOW-Bs2 to monitor its expression and eventually binding. Two different strategies were used as described in materials and methods section *1.2.13* and *1.2.17* to design the construct that would express OxyR fused with pGLOW-Bs2.

1.4.2.I Strategy 1 for approach 2. Strategy 1 involved replacement of the sequence encoding HaloTag from plasmid DNA V3080 with the sequence encoding pGLOW-Bs2. For this purpose, pGLOW-Bs2-Stop(pUC18) vector bought from the company was reconstructed as mentioned in section *1.2.13*. Xhoi/EcoRi double digestion was carried out on the re-constructed pUC18 construct and on the plasmid DNA V3080 (Refer section *1.2.14* for details). Figure 16 shows the digestion reactions ran on a 1% Agarose gel. V3080, when digested, showed two bands, one of about 1000 bp in size indicated digested HaloTag sequence and the other of about 4086 bp in size indicated the digested vector. The band indicating a digested vector (Figure 16, lane 1) was excised and extracted from the gel to use for ligation with the insert. On digestion, the re-constructed pUC18 vector also showed two bands, the one having the size of about 3900 bp indicated the digested pUC18 vector and the one of size of about 400 bp indicated the digested pGLOW-Bs2 sequence (Figure 16, lane 2). This band of size 400 bp is the insert that needed to be cloned in digested V3080. This band was also excised and extratcted. A ligation reaction was set as described in section *1 2.15* using the gel extracted acceptor vector and insert. After colony screening, the plasmid DNAs isolated were sent for sequencing. The sequencing results (not included) indicated that the pGLOW-Bs2 was present downstream and in frame with the *P. gingivalis* OxyR present in construct V3080. Ideally this construct was expected to express the *P. gingivalis* OxyR as a fusion protein with the pGLOW-Bs2, resulting in emission of a cyan-green fluorescence after protein expression. To check the fluorescence, this construct was transformed in *E. coli* expression cells and the culture slide was prepared as mentioned in section *1.2.15* to observe it under the fluorescence microscope.

No cyan green fluorescence was observed (Images not included). The reason for this could be either the fusion protein was not expressed or the fluorescent protein Bs2 was not able

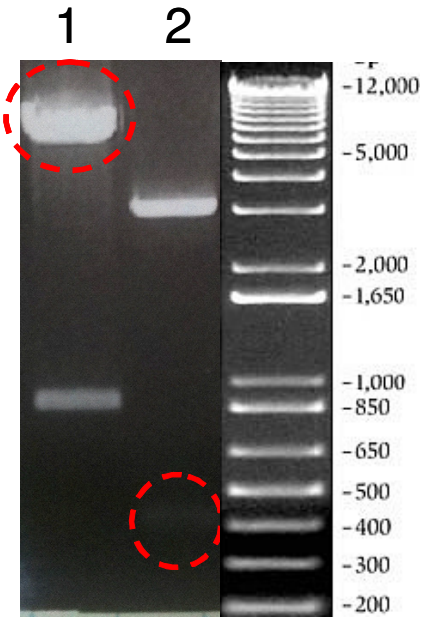

Figure 16. Agarose gel showing plasmid DNA V3080 (Lane 1) and the re-constructed pUC18 vector (Lane 2) digested with

to achieve a proper conformation after expression. For emitting fluorescence, conformation of the fluorescent protein is critical. Even though it is expressed as a fusion protein, care must be taken to allow the two proteins to fold independently. With this goal, strategy 2 was applied to make the fusion protein.

1.4.2.II. Strategy 2 for approach 2. Studies showed that a truncated YtvA that consists of only photoreceptor domain, forms a stable homodimer in solution[79]. Hence it was decided to incorporate a ribosomal binding site (RBS) in between OxyR and the sequence encoding pGLOW-Bs2 which will be cloned in frame with the OxyR downstream of OxyR. This incorporation might help pGLOW-Bs2 to fold independently as a dimer and once properly folded pGLOW-Bs2 should emit cyan-green fluorescence. Keeping this concept in mind, three constructs were designed as mentioned in materials and methods section *1.2.17*.

Three inserts which were to be cloned in these three constructs were amplified from pGLOW-Bs2-Stop(pUC18) using primer pairs FP1-RP (for two amplifications) and FP2-RP (for one amplification) as mentioned in section *1.2.18* and were run on 2% agarose gel to check the amplification (Figure 17A). All the three inserts should have a size of around 415 bp. An undesired band of 3kb was also observed in all the samples. Hence the band of desired size (450 bp) was gel purified for all the three samples. The gel purified inserts were used to set digestion with restriction enzymes Xhoi/EcoRi.

Acceptor vectors V3107 and V3080 were digested with Xhoi/EcoRi and ran in a gel to excise the desired band. (Figure 17 B). A DNA piece encoding Halotag protein was cut due to digestion by enzymes Xhoi and EcoRi as indicated by a band of size 1000 bp on the gel, for each plasmid DNA. The bigger band indicates the digested acceptor vector piece. The bigger bands for each vector were excised and gel extracted. The gel extracted acceptor vectors were used to

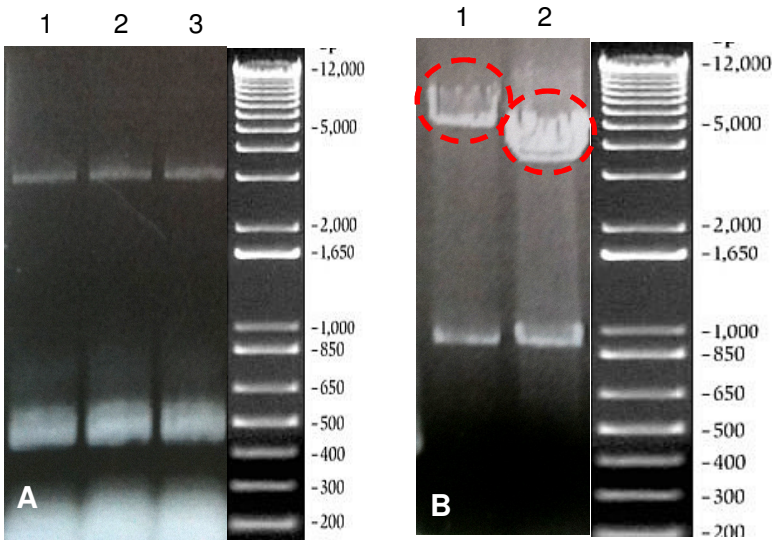

Figure 17A. Agarose gel to check the amplification of pGLOW-Bs2 inserts, where Lane 1, 2 – Inserts amplified with primer pair FP1-RP, Lanes 3 – Insert amplified with primer pair FP2-RP.
Figure 17B. Vectors V3080 (lane 1) and V3107 (lane 2) digested with Xhoi and EcoRi

set ligation reactions. Three ligation reactions were set to make constructs ***P***, ***Q*** and ***R*** as mentioned in section *1.2.18* and section *1.2.15*.

Plasmid DNAs isolated from many samples after colony screening, were sent for sequencing. Figure 18 A and B are examples of the sequencing results obtained. Sequencing results indicated that for all the three ligation reactions the desired constructs were not obtained. In most of the cases some totally different sequence had got inserted downstream the Xhoi recognition sequence as indicated in figure 18A and 18B. From the trend observed in the sequencing results it was concluded that some undesirable sequences were getting amplified as inserts. Hence, it was necessary to check the inserts by sequencing before cloning downstream OxyR present in vectors V3080 and V3107. To achieve this purpose, strategy 3 was applied.

1.4.2.III. Strategy 3 for approach 2. The final aim of this strategy is to obtain constructs ***P***,***Q*** and ***R*** mentioned in strategy 2 but strategy 3 involves one additional step of cloning the amplified inserts into a PCR vector to check the amplified sequence, before cloning the inserts into Flexi vectors. For this purpose, PCR vector TOPO2.1 (Invitrogen) was used as mentioned in section *1.2.19*.

After TOPO cloning and transformation colonies were screened and plasmid DNAs were sent for sequencing. Figure 19 A shows the sequence of the insert amplified with primer pair FP1-RP cloned into TOPO2.1 vector (Named as **P1**). This sequence indicated that a full length Bs2, along with its stop codon had got cloned into TOPO vector. All the new upstream-downstream sequences that were inserted, for example, Xhoi recognition sequence, EcoRi site and *E. coli* RBS were present at the right place. Figure 19 B shows the sequence for the insert amplified with primer pair FP2-RP and cloned into TOPO vector (Named as **P2**). For this cloning also sequence was as expected, with Xhoi, EcoRi recognition sequences, *P. gingivalis*

A

NNNNNNNNNNCGNNNNTCGTGACNGTTGNNGGCTTGCTGCGTTCGGCCGTCCCATCGGATATGCACAAGTTGCAGACAGG
GCAGCATTTGGCTGTTTCT**CTCGAG**CCAACCACTGAGGATCTGTACTTTCAGAGCGATAACGATGGATCCGAAATCGGTACT
GGCTTTCCATTCGACCCCCATTATGTGGAAGTCCTGGGCGAGCGCATGCACTACGTCGATGTTGGTCCGCGCGATGGCACC
CCTGTGCTGTTCCTGCACGGTAACCCGACCTCCTCCTACGTGTGGCGCAACATCATCCCGCATGTTGCACCGACCCATCGCT
GCATTGCTCCAGACCTGATCGGTATGGGCAAATCCGACAAACCAGACCTGGGTTATTTCTTCGACGACCACGTCCGCTTCAT
GGATGCCTTCATCGAAGCCCTGGGTCTGGAAGAGGTCGTCCTGGTCATTCACGACTGGGGCTCCGCTCTGGGTTTCCACTG
GGCCAAGCGCAATCCAGAGCGCGTCAAAGGTATTGCATTTATGGAGTTCATCCGCCCTATCCCGACCTGGGACGAATGGCC
AGAATTTGCCCGCGAGACCTTCCAGGCCTTCCGCACCACCGACGTCGGCCGCAAGCTGATCATCGATCAGAACGT

B

NNNNNNNNNNNGCTATGAGCAGCTGGCAGAGGCCATCCGCGCAAGANTGGATGGCCATTTCGATAAAGTTTTAAAACAGG
CGGTTGTTTTGCNGGAGGGTAGCACTGAGGCTCTGCTGCCAGCGCTGGCTGTGCCGGATCAGCGCNNACGTANTGGGGTT
GNTTNCTGCCGTGCATTGTGCCGGAACCGCGCCANACTATGGGCCTGGTCGATGTTGGTCCGCGCGATGGCACCCCTGTGC
TGTTCCTGCACGGTAACCCGACCTCCTCCTACGTGTGGCGCAACATCATCCCGCATGTTGCACCGACCCATCGCTGCATTGC
TCCAGACCTGATCGGTATGGGCAAATCCGACAAACCAGACCTGGGTTATTTCTTCGACGACCACGTCCGCTTCATGGATGCC
TTCATCGAAGCCCTGGGTCTGGAAGAGGTCGTCCTGGTCATTCACGACTGGGGCTCCGCTCTGGGTTTCCACTGGGCCAAG
CGCAATCCAGAGCGCGTCAAAGGTATTGCATTTATGGAGTTCATCCGCCCTATCCCGACCTGGGACGAATGGCCAGAATTTG
CCCGCGAGACCTTCCAGGCCTTCCGCACCACCGACGTCGGCCGCAAGCTGATCATCGA.....

Figure 18A. Sequencing result obtained after cloning pGLOW-Bs2 downstream *P. gingivalis* OxyR present in Flexi vector where blue, bold letters indicate the end part of the sequence of *P. gingivalis* OxyR

Figure 18B. Sequencing result obtained after cloning pGLOW-Bs2 downstream *E. coli* OxyR present in Flexi vector where blue, bold letters indicate the end part of the sequence of *E. coli* OxyR

A

TOPO2.1.....AATTCGGCTTGAGCT**CTCGAG**TG**AGGAGA**T**ATGGCGTCGTTCCAGTCGTTCGGCATCCCGGGCCAGCTGGAA**
GTCATCAAGAAGGCGCTGGATCACGTGCGCGTCGGCGTGGTCATCACCGATCCCGCGCTGGAAGATAACCCGATCGTCTA
CGTGAACCAGGGCTTCGTGCAGATGACCGGCTACGAGACCGAGGAAATCCTGGGCAAGAACGCGCGCTTCCTCCAGGGG
AAGCACACCGATCCGGCGGAAGTGGACAACATCCGCACCGCGCTGCAAAATAAAGAACCGGTCACCGTGCAGATCCAGA
ACTACAAGAAGGACGGCACGATGTTCTGGAACGAACTGAACATCGATCCGATGGAAATCGAGGATAAGACGTATTTCGTC
GGCATCCAGAACGACATCACCAAGCAGAAGGAATATGAAAAGCTGCTTGAATGAGAATTC**AGTCAG**AAGCCGA
.....**TOPO 2.1**

B

TOPO2.1.....NCGAGCTCGGATCCNCTAGTAACGGCCGCCAGTGTGCTGGAATTCGGCTTGAGCT**CTCGAG**AAAT**AAGAAA**CA
ATT**ATGGCGTCGTTCCAGTCGTTCGGCATCCCGGGCCAGCTGGAAGTCATCAAGAAGGCGCTGGATCACGTGCGCGTCGG**
CGTGGTCATCACCGATCCCGCGCTGGAAGATAACCCGATCGTCTACGTGAACCAGGGCTTCGTGCAGATGACCGGCTACG
AGACCGAGGAAATCCTGGGCAAGAACGCGCGCTTCCTCCAGGGGAAGCACACCGATCCGGCGGAAGTGGACAACATCCG
CACCGCGCTGCAGAATAAAGAACCGGTCACCGTGCAGATCCAGAACTACAAGAAGGACGGCACGATGTTCTGGAACGAA
CTGAACATCGATCCGATGGAAATCGAGGATAAGACGTATTTCGTCGGCATCCAGAACGACATCACCAAGCAGAAGGAATA
TGAAAAGCTGCTTGAATGA**GAATTCAGTCAG**AAGCCGAATTCTGC...**TOPO 2.1**

Figure 19A. Sequence of vector P1 (Bs2 amplified with primer pair FP1-RP cloned in TOPO2.1 PCR vector), where Green, bold, underlined letters - the sequence of Bs2, Pink, bold, underlined letters - recognition sequences of Xhoi, EcoRi, Dark pink, bold, underlined letters – sequence for *E. coli* RBS, Red, bold, underlined letters – stop codon, pink letters – primer sequences, Black letters- sequence from TOPO vector.
Figure 19B. Sequence of vector P2 (Bs2 amplified with primer pair FP2-RP cloned in TOPO2.1 PCR vector), where Green, bold, underlined letters - the sequence of Bs2, Pink, bold, underlined letters - recognition sequences of Xhoi, EcoRi, Dark pink, bold, underlined letters – sequence for *P. gingivalis* RBS, Red, bold, underlined letters – stop codon, pink letters – primer sequences, Black letters- sequence from TOPO vector

RBS, full length Bs2 and stop codon all present at the expected location. Sequencing of the cloned TOPO vectors confirmed that the inserts to be cloned into flexi vectors were having the expected sequences.

Hence the next step was digestion of TOPO vectors P1, P2 and acceptor vectors V3107, V3080 with Xhoi and EcoRi. After the incubation for digestion was over, all the digested vectors were run Agarose gel. Figure 20A shows the acceptor vectors V3080 and V3107 digested with Xhoi, EcoRi in lanes 1 and 2 respectively, indicated HaloTag protein coding sequence which is digested out from the vector. The bigger bands in both the lanes indicated the digested acceptor vectors.

These bands were gel extracted using Quiagen gel extraction kit and used for ligation.

Figure 20 B shows the digested constructs P1 and P2 run on a 2% Agarose gel. Both the constructs showed a band of size around 450 bp indicating insert which was digested out from the TOPO vector and a band of size 3.9 kb indicating digested TOPO vector. The bands for digested insert for both the constructs were excised from the gel and extracted. They were used for ligation.

Insert from P1 was ligated with digested vector V3107 to make construct ***P***, and with digested vector V3080 to make construct ***Q***. Insert from P2 was ligated with digested vector V3080 to make construct ***R***. Ligation reactions were set as mentioned in step 4 of strategy 2.

For all the three ligation reactions plasmid DNAs were sent for sequencing after colony screening. Sequence for construct ***P*** was exactly as designed (Figure 21A). Hence construct ***P*** is ready to be transformed into *EC BL21(DE3)* expression cells to monitor expression of *EC* OxyR expressed as a fusion protein with pGLOW-Bs2 under fluorescent microscope. The construct can also be utilized to visualize *EC* OxyR-DNA binding as mentioned in future directions.

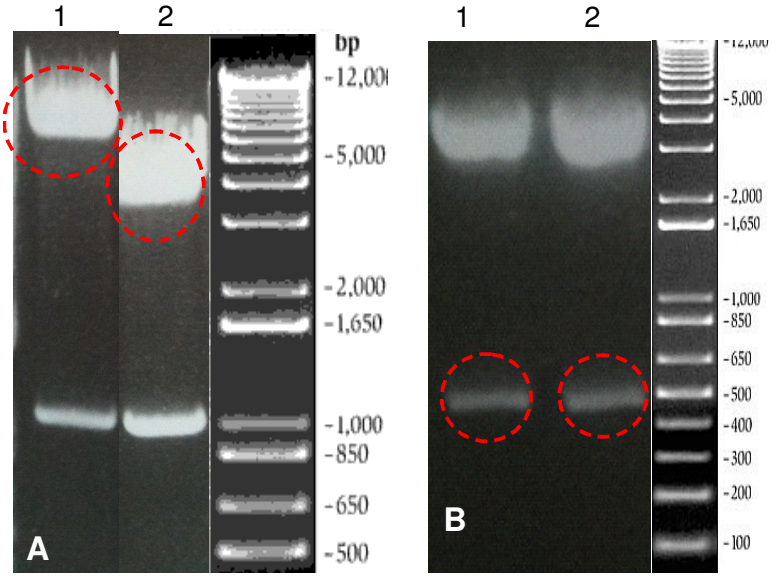

Figure 20A. Vectors V3080 (lane 1) and V3107 (lane 2) again digested with Xhoi and EcoRi.
Figure 20B. Construct P1 (lane 1) and construct P2 (Lane 2) digeted with Xhoi and EcoRi.

A

NTGAGCAGCTGGCAGAGGCCATCCGCGCAAGAATGGATGGCCATTTCGATAAAGTTTTAAAACAGGCG
GTTGTTTCTCTCGAGTGAGGAGATATGGCGTCGTTCCAGTCGTTCGGCATCCCGGGCCAGCTGGAAGTCA
TCAAGAAGGCGCTGGATCACGTGCGCGTCGGCGTGGTCATCACCGATCCCGCGCTGGAAGATAACCCGA
TCGTCTACGTGAACCAGGGCTTCGTGCAGATGACCGGCTACGAGACCGAGGAAATCCTGGGCAAGAACG
CGCGCTTCCTCCAGGGGAAGCACACCGATCCGGCGGAAGTGGACAACATCCGCACCGCGCTGCAAAATA
AAGAACCGGTCACCGTGCAGATCCAGAACTACAAGAAGGACGGCACGATGTTCTGGAACGAACTGAACAT
CGATCCGATGGAAATCGAGGATAAGACGTATTTCGTCGGCATCCAGAACGACATCACCAAGCAGAAGGAA
TATGAAAAGCTGCTTGAATGAGAATTCTAGAGTCGACCTGCAGGCATGCAAGCTGATCCGGCTGCTAACA
AAGCCCGAAAGGAAGCTGAGTTGGCTGCTGCCACCGCTGAGCAATAACTAGCATAACCNA

B

GTGACNGTTGATTGGCTTGCTGCGTTCGGCCGTCCCATCGGATATGCACAAGTTGCAGACAGGGCAGCA
TTTGGCTGTTTCTCTCGAGTGAGGAGATATGGCGTCGTTCCAGTCGTTCGGCATCCCGGGCCAGCTGGAA
GTCATCAAGAAGGCGCTGGATCACGTGCGCGTCGGCGTGGTCATCACCGATCCCGCGCTGGAAGATAAC
CCGATCGTCTACGTGAACCAGGGCTTCGTGCAGATGACCGGCTACGAGACCGAGGAAATCCTGGGCAAG
AACGCGCGCTTCCTCCAGGGGAAGCACACCGATCCGGCGGAAGTGGACAACATCCGCACCGCGCTGCAA
AATAAAGAACCGGTCACCGTGCAGATCCAGAACTACAAGAAGGACGGCACGATGTTCTGGAACGAACTGA
ACATCGATCCGATGGAAATCGAGGATAAGACGTATTTCGTCGGCATCCAGAACGACATCACCAAGCAGAA
GGAATATGAAAAGCTGCTTGAATGAGAATTCGAGCTCGGTA

C

NNTTCGTGACNGTTGATTGGCTTGCTGCGTTCGGCCGTCCCATCGGATATGCACAAGTTGCAGACAGGG
CAGCATTTGGCTGTTTCTCTCGAGAAATAAGAAACAATTATGGCGTCGTTCCAGTCGTTCGGCATCCCGG
GCCAGCTGGAAGTCATCAAGAAGGCGCTGGATCACGTGCGCGTCGGCGTGGTCATCACCGATCCCGCGC
TGGAAGATAACCCGATCGTCTACGTGAACCAGGGCTTCGTGCAGATGACCGGCTACGAGACCGAGGAAAT
CCTGGGCAAGAACGCGCGCTTCCTCCAGGGGAAGCACACCGATCCGGCGGAAGTGGACAACATCCGCAC
CGCGCTGCAGAATAAAGAACCGGTCACCGTGCAGATCCAGAACTACAAGAAGGACGGCACGATGTTCTGG
AACGAACTGAACATCGATCCGATGGAAATCGAGGATAAGACGTATTTCGTCGGCATCCAGAACGACATCAC
CAAGCAGAAGGAATATGAAAAGCTGCTTGAATGAGAATTCAGTCAGAAGCC

Figure 21A. Sequence of construct ***P*** where, where Blue, blue letters – Sequence from the end part of *E. coli* OxyR, Green, bold, letters - the sequence of Bs2, Pink, bold, underlined letters - recognition sequences of Xhoi, EcoRi, Dark pink, bold, underlined letters – sequence for *E. colis* RBS, Red, bold, underlined letters – stop codon, pink letters – primer sequences, Black letters- sequence from Flexi vector.

Figure 21B. Sequence obtained while making construct ***Q*** where, where Blue, blue letters – Sequence from the end part of *P. gingivalis* OxyR, Green, bold, letters - the sequence of Bs2, Pink, bold, underlined letters - recognition sequences of Xhoi, EcoRi, Dark pink, bold, underlined letters – sequence for *E. coli* RBS, Red, bold, underlined letters – stop codon, pink letters – primer sequences.

Figure 21C. Sequence obtained while making construct ***R*** where, Blue, blue letters – Sequence from the end part of *P. gingivalis* OxyR, Green, bold, letters - the sequence of Bs2, Pink, bold, underlined letters - recognition sequences of Xhoi, EcoRi, Dark pink, bold, underlined letters – sequence for *P. gingivalis* RBS, Red, bold, underlined letters – stop codon, pink letters – primer sequences.

Sequences for constructs ***Q*** and ***R*** were not totally as expected as the sequence downstream of the inserted Bs2, was weird (Figure 21B, 21C). It was not matching with the sequence from the Flexi vector downstream of the EcoRi recognition sequence in Flexi vector. Although Bs2 was in frame with OxyR and every other aspect of the sequence is perfect, construction of ***Q*** and ***R*** is not complete due to the weird downstream sequences. Digestion and ligation needs to be repeated on these samples to get constructs ***Q*** and ***R***.

1.4.3. Making a positive control construct. In all the earlier constructs made pGLOW-Bs2 was expressed as a fusion protein tagged at the C-terminus of OxyR. The expression and fluorescence from those constructs is dependent on expression of OxyR. An experimental positive control whose fluorescence is independent of OxyR-expression was needed. To prepare that pGLOW-Bs2 alone needed to be expressed using pFC20K Halo Tag T7 SP6 Flexi Vector. Cloning and ligation was done as mentioned in section *1.2.20*.

Figure 22 shows the sequencing result. It indicates that the full length (411 bp) pGLOW-Bs2 along with its stop codon is present downstream the T7 promoter in Flexi vector. According to the sequencing results obtained (Figure 22) pGLOW-Bs2-Stop downstream of the T7 promoter and hence should be expressed when IPTG was added. Hence it was expected to see a cyan-green fluorescence spread over the entire area of the cells. Culture slide was prepared as mentioned in section *1.2.21*. No true fluorescence was observed. The cyan-green fluorescence in the negative control culture was of same intensity. In fact for both the negative control culture and the positive control cultures the fluorescence intensity observed under all the fluorescent filters was the same. (Images not captured). These observations were consistent for all the three cultures induced with different concentrations of IPTG.

CCGACTCAGTGACTATAGATAAGGAGCGATCGCC**ATGGCGTCGTTCCAGTCGTTCGGCATC**
CCGGGCCAGCTGGAAGTCATCAAGAAGGCGCTGGATCACGTGCGCGTCGGCGTGGTCATC
ACCGATCCCGCGCTGGAAGATAACCCGATCGTCTACGTGAACCAGGGCTTCGTGCAGATG
ACCGGCTACGAGACCGAGGAAATCCTGGGCAAGAACGCGCGCTTCCTCCAGGGGAAGCA
CACCGATCCGGCGGAAGTGGACAACATCCGCACCGCGCTGCAAAATAAAGAACCGGTCAC
CGTGCAGATCCAGAACTACAAGAAGGACGGCACGATGTTCTGGAACGAACTGAACATCGA
TCCGATGGAAATCGAGGATAAGACGTATTTCGTCGGCATCCAGAACGACATCACCAAGCA
GAAGGAATATGAAAAGCTGCTCGAGTGAGTTTCTCT

Figure 22. Sequencing result of the positive control vector constructed using Flexi vector, where green letters – sequence encoding pGLOW-Bs2, red letters – stop codon, black letters – sequence from the Flexi vector.

1.4.4. Checking company's expression vector for fluorescence. As the positive control expression vector made in the lab was not emitting any fluorescence, pGLOW-Bs2 cloned in an expression vector (pGLOW-K^{XN}-Bs2) was bought from 'evocatal'. This expression vector was used to check if pGLOW-Bs2 expressed from this vector is emitting fluorescence. This vector was transformed in *E. coli BL21(DE3)* expression cells (Invitrogen). The procedure mentioned in section *1.2.21* was repeated for growing the culture and protein expression. A culture for strain V3080 was used as negative control. The slides were observed under the fluorescent microscope and fluorescence intensity was checked under all the fluorescent filters like CFP, DAPI, GFP, and DsRed. The camera settings were as mentioned in section *1.2.22.* The images were captured for the slides prepared from the cultures induced with 1mM IPTG (Figure 23).

Again no intense fluorescence was observed for CFP. In fact for both the negative control culture and the positive control cultures the fluorescence intensity observed under all the fluorescent filters was the same. These observations were consistent for all the three cultures induced with different concentrations of IPTG.

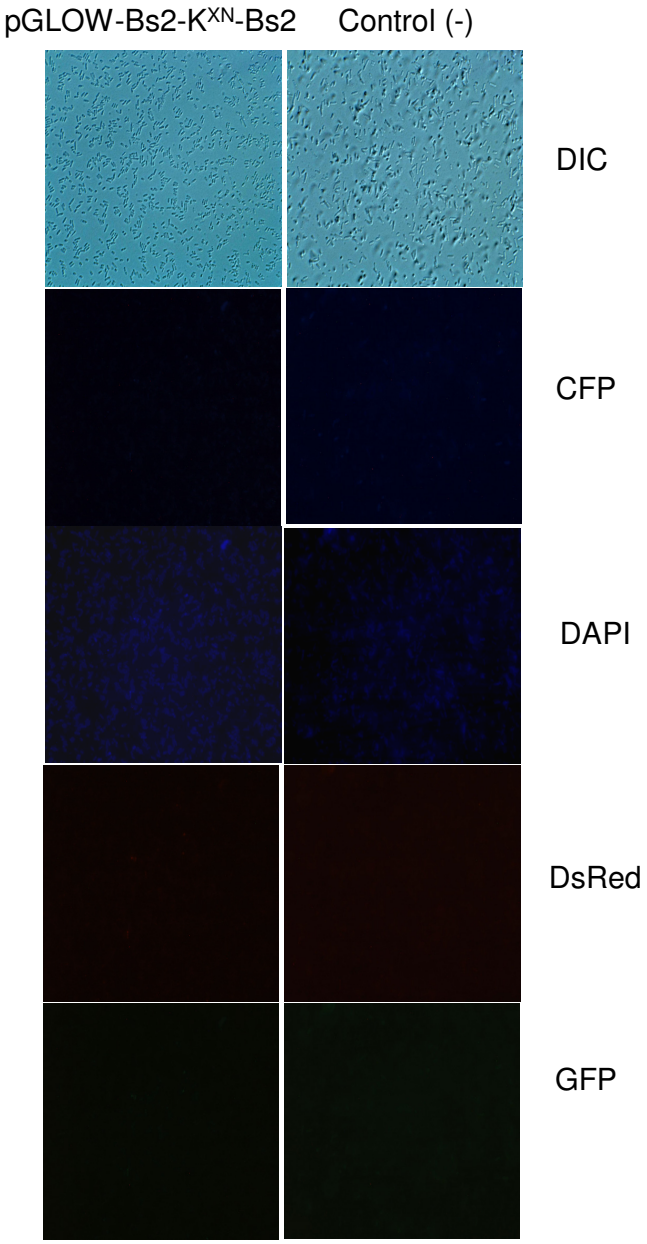

Figure 23. Images captured to check fluorescence after expression from construct pGLOW-Bs2-KXN-Bs2 and from construct V3080 (negative control).

1.6. Discussion

In vitro characterization of binding started with CHIP-chip assay. This assay provided a list of target binding fragments for *P. gingivalis* OxyR (Refer table 1). These were different than those predicted in literature. The reason behind this discrepancy could be the difference in assay conditions. CHIP-chip assay was carried out in completely anaerobic conditions, whereas the fragments that are predicted binding sites for OxyR in literature are found under oxidative stress conditions[62]. Hence, while performing EMSAs, fragments provided by CHIP-chip assay, microarray studies as well as those mentioned in the literature are used.

At first, in vivo expressed and purified *P. gingivalis* OxyR was used for EMSAs. The very first purification process gave a protein of 50 kDa under denaturing, non-reducing conditions (Figure 2). The size of the full length OxyR is 35 kDa. Hence appearance of a band of 50 kDa raised a question whether the protein is full length. There are two possibilities for appearance of this 50 kDa band. One possibility is that the purified, full length protein has formed an intra-molecular disulphide bond which is giving the protein a larger appearance. Other possibility is that the N-terminal domain has been cleaved by proteases and the dimer of the regulatory domain which has a size of about 25 kDa is responsible for the band of 50 kDa. This protein preparation did not bind with the tarhet DNA fragments during EMSAs. Absence of binding points towards the second possibility, indicating the absence of the N-terminal DNA binding domain in the purified preparation.

When a fresh batch of *P. gingivalis* OxyR was simultaneously expressed in vivo and purified along with *E. coli* OxyR both the proteins showed a band of about 37 kDa indicating that a full length protein is present in the purified preparation (Figure 12). During this purification process some more protease inhibitors were used than the first purification process.

This might be the reason behind purification of the full length protein. But this full length *P. gingivalis* OxyR never bound to the target fragments whereas *E. coli* OxyR did bind. The binding of *E. coli* OxyR with the fragments which are the predicted binding sites for *P. gingivalis* OxyR is not surprising as both the proteins are the members of LysR family where the members display high conservation in the N-terminal DNA binding domain[40,41]. These EMSAs indicated that in vivo expressed and purified *P. gingivalis* OxyR may not be stable and hence was not able to bind with the DNA fragments *in vitro*. While the *in vivo* expressed and purified *E. coli* OxyR bound to its own target fragment as well as to the target fragment for *P. gingivalis* OxyR.

In vitro made and purified *P. gingivalis* OxyR also showed a band of 50 kDa after purification again indicating that N-terminal DNA binding domain has been cleaved and the band of 50 kDa is the dimer of the regulatory domain (Figure 3). There was one modification in the purification process when *in vitro* protein was purified. After addition of TEV protease, the elution was not applied to the His-link resin to remove TEV protease, instead 5 mM Zn^{2+} was added to inactivate the un-removed TEV-Protease. As application of the elution to His-link resin was skipped, it might resulted in retention of the cleaved N-terminal DNA binding domain in the purified preparation which showed a band at 15 kDa (Figure 3). May be the presence of this cleaved DNA binding domain in the preparation resulted in binding of this preparation to the target fragments used (Figures 7, 8, 9). Presence of zinc ion in this preparation is also notable. As the mutant *P. gingivalis* OxyR proteins made in vitro were not able to bind with the same target fragments the residues mutated might have a crucial role in OxyR-DNA binding. EDTA treatment was capable of abrogating the binding, zinc which was present in this preparation might had a role in binding.

The HaloTag TMRDirect ligand was useful to monitor the expression of P. gingivalis OxyR but was not totally suitable for further investigation due to the pitfalls observed. Hence use of FMN-based fluorescent protein was theoretically ideal to make a fusion protein with OxyR. As we never got any fluorescence emission it is necessary first to check the expression and fluorescence of the pGLOW-Bs2 protein itself. Western blot can be used to check the expression. The expressed fluorescent protein can be run on a native gel to check if the band is fluorescent. Then various constructs can be made using that to make a fusion protein that will be fluorescent.

Appendix I

List of primers 1.

1. PG0964F – 5’- GGTCATTTTATCGCAGCCTA -3’
   PG0964R – 5’ –GAGCGGAGCATGATTTTAGC
   Fragment size – 1038 bp

2. PG 0360F- 5’-ATCGCCGGTCAGCATAGAGT-3’
   PG0360R – 5’-ATCATTCGCAAGAGCGAAAA-3’
   Fragment size - 918bp

3. PG1307F – 5’-AAAGGCTGTCCGCACTCAT-3’
   PG1307R – 5’-GGTGAACATCTTTACTTCTGTCGTT-3’
   Fragment size - 993bp

4. PG0304F – 5’- AACAAGGACAAAGGCGGTGT -3’
   PG0304HR – 5’- CATGGTCGCTCGTCAGATAA-3’
   Fragment size - 830bp

5. PG1240F – 5’- TCGATGTAGCACGTCAGCTC-3’
   PG1240R – 5’- CACTTTCACTTCCAATCTCTTCTTC-3’
   Fragment size - 636bp

6. PG1240IFF – 5’- CGATATGTATGTCCGCGAAG-3’
   PG1240IFR – 5’- GATGAGCTGTCCCCTTTCAA-3’
   Fragment size - 947bp

7. PG1862IFF- TGATTATCCCATAAAGGGTGAGA-3’
   PG1862IFR- ACCATTCTCGGAGCCTTGTA-3’
   Fragment size - 601bp

8. hmuF - 5’-GCACCTGTTTATTGAGCAAAG-3’
   hmuR – 5’-TCCCAGTTCAAATCGTTCTT-3’
   Fragment size - 500bp

9. rbr F – 5’- GAGGTCGACTCTTTGTGTTCC-3’
   rbrR – 5’- TGAGGTGGACTCTTTGTGTTC-3’
   Fragment size - 200bp

10. sod1F – 5’- TGAACAATAAGACGAACTCCTTGTTTT-3’
    sod1R -5’- GCTTCATAATTCGGCTCTTGA-3’
    Fragment size - 1000bp

11. sod2F – 5'-AAGACGAACTCCTTGTTTTGAGAA-3'
    sod2R – 5'-GCTTCATAATTCGGCTCTTGA-3'
    Fragment size - 1000bp

12. sod3F – 5'-TCAACGAAATGGTCTTGCTG-3'
    sod3R – 5'- GCTTCATAATTCGGCTCTTGA-3'
    Fragment size – 1000bp

13. PGahpc1 F- 5'-CAGTCGATTGACAATGAAATCTCC-3'
    PGahpc1 R- 5'-GTATGAACGTTTGTTTCAGGTG-3'
    Fragment size - 140 bp

14. FP pg upstream ahpc – 5' - CTGTCAAAGCATATGTTCAGATG - 3'
    RP pg upstream ahpc - GAACGTTTGTTTCAGGTGC
    Fragment size - 550bp

References.

(1) Brown, L. R.; Dreizen, S. *Archives of the Foundation of Thanatology* **1975**, *5*, 142-142.

(2) Schiott, C. R. *Journal of Periodontal Research* **1973**, 7-10.

(3) Aas, J. A.; Paster, B. J.; Stokes, L. N.; Olsen, I.; Dewhirst, F. E. *Journal of Clinical Microbiology* **2005**, *43*, 5721-5732.

(4) Paster, B. J.; Boches, S. K.; Galvin, J. L.; Ericson, R. E.; Lau, C. N.; Levanos, V. A.; Sahasrabudhe, A.; Dewhirst, F. E. *Journal of Bacteriology* **2001**, *183*, 3770-3783.

(5) Dewhirst, F. E.; Chen, T.; Izard, J.; Paster, B. J.; Tanner, A. C. R.; Yu, W.-H.; Lakshmanan, A.; Wade, W. G. *Journal of Bacteriology* **2010**, *192*, 5002-5017.

(6) Govoni, M.; Jansson, E. A.; Weitzberg, E.; Lundberg, J. O. *Nitric Oxide-Biology and Chemistry* **2008**, *19*, 333-337.

(7) Srinivasan, N. *Innate Immunity* **2010**, *16*, 391-404.

(8) Cosseau, C.; Devine, D. A.; Dullaghan, E.; Gardy, J. L.; Chikatamarla, A.; Gellatly, S.; Yu, L. L.; Pistolic, J.; Falsafi, R.; Tagg, J.; Hancock, R. E. W. *Infection and Immunity* **2008**, *76*, 4163-4175.

(9) Lamont, R. J.; Jenkinson, H. F. *Microbiology and Molecular Biology Reviews* **1998**, *62*, 1244-+.

(10) Albandar, J. M.; Brunelle, J. A.; Kingman, A. *Journal of Periodontology* **1999**, *70*, 13-29.

(11) Listgarten, M. A. *Journal of Clinical Periodontology* **1986**, *13*, 418-425.

(12) Crich, A. *Canadian Medical Association journal* **1932**, *26*, 662-5.

(13) Migliari, D. A.; Sugaya, N. N.; Mimura, M. A.; Cuce, L. C. *Revista do Instituto de Medicina Tropical de Sao Paulo* **1998**, *40*, 15-18.

(14) Matsuo, T.; Nakagawa, H.; Matsuo, N. *Ophthalmologica* **1995**, *209*, 109-111.

(15) Schroeder, H. E. *Journal of Clinical Periodontology* **1986**, *13*, 426-430.

(16) Savage, A.; Eaton, K. A.; Moles, D. R.; Needleman, I. *Journal of Clinical Periodontology* **2009**, *36*, 458-467.

(17) D'Aiuto, F.; Parkar, M.; Andreou, G.; Suvan, J.; Brett, P. M.; Ready, D.; Tonetti, M. S. *Journal of Dental Research* **2004**, *83*, 156-160.

(18) Nibali, L.; D'Aiuto, F.; Griffiths, G.; Patel, K.; Suvan, J.; Tonetti, M. S. *Journal of Clinical Periodontology* **2007**, *34*, 931-937.

(19) Paraskevas, S.; Huizinga, J. D.; Loos, B. G. *Journal of Clinical Periodontology* **2008**, *35*, 277-290.

(20) Noble, J. M.; Borrell, L. N.; Papapanou, P. N.; Elkind, M. S. V.; Scarmeas, N.; Wright, C. B. *Journal of Neurology Neurosurgery and Psychiatry* **2009**, *80*, 1206-1211.

(21) Kaye, E. K.; Valencia, A.; Baba, N.; Spiro, A.; Dietrich, T.; Garcia, R. I. *Journal of the American Geriatrics Society* **2010**, *58*, 713-718.

(22) Pussinen, P. J.; Alfthan, G.; Jousilahti, P.; Paju, S.; Tuomilehto, J. *Atherosclerosis* **2007**, *193*, 222-228.

(23) Ford, P. J.; Gemmell, E.; Timms, P.; Chan, A.; Preston, F. M.; Seymour, G. J. *Journal of Dental Research* **2007**, *86*, 35-40.

(24) Beck, J. D.; Eke, P.; Heiss, G.; Madianos, P.; Couper, D.; Lin, D. M.; Moss, K.; Elter, J.; Offenbacher, S. *Circulation* **2005**, *112*, 19-24.

(25) Zadik, Y.; Bechor, R.; Galor, S.; Levin, L. *British Dental Journal* **2010**, *208*.

(26) Kuo, L. C.; Poison, A. M.; Kang, T. *Public Health* **2008**, *122*, 417-433.

(27) Dowsett, E. B. *Proceedings of the Royal Society of Medicine* **1924**, *17*, 6-8.

(28) Spottel, W. *Zool Anzeiger* **1927**, *71*, 303-331.

(29) Imrie, D. A. *Proceedings of the Royal Society of Medicine* **1928**, *22*, 74-5.

(30) Allenspachpetrzilka, G. E.; Guggenheim, B. *Journal of Clinical Periodontology* **1983**, *10*, 609-617.

(31) Helderman, W. H. V. *Journal of Clinical Periodontology* **1981**, *8*, 261-280.

(32) Saxe, S. R.; Greene, J. C.; Bohannan, H. M.; Vermilli.Jr *Periodontics* **1967**, *5*, 217-&.

(33) Loe, H.; Theilade, E.; Jensen, S. B. *Journal of Periodontology* **1965**, *36*, 177-&.

(34) Loesche, W. J.; Syed, S. A. *Infection and Immunity* **1978**, *21*, 830-839.

(35) Gibbons, R. J.; Berman, K. S.; Knoettne.P; Kapsimal.B *Archives of Oral Biology* **1966**, *11*, 549-&.

(36) Slots, J.; Ting, M. *Periodontology 2000* **1999**, *20*, 82-121.

(37) Ali, R. W.; Lie, T.; Skaug, N. *Journal of Periodontology* **1992**, *63*, 540-547.

(38) Lin, X.; Wu, J.; Xie, H. *Infection and Immunity* **2006**, *74*, 6011-6015.

(39) Lewis, J. P. *Periodontology 2000* **2010**, *52*, 94-116.

(40) Henikoff, S.; Haughn, G. W.; Calvo, J. M.; Wallace, J. C. *Proceedings of the National Academy of Sciences of the United States of America* **1988**, *85*, 6602-6606.

(41) Schell, M. A. *Annual Review of Microbiology* **1993**, *47*, 597-626.

(42) Stragier, P.; Patte, J. C. *Journal of Molecular Biology* **1983**, *168*, 333-350.

(43) Stec, E.; Witkowska-Zimny, M.; Hryniewicz, M. M.; Neumann, P.; Wilkinson, A. J.; Brzozowski, A. M.; Verma, C. S.; Zaim, J.; Wysocki, S.; Bujacz, G. D. *Journal of Molecular Biology* **2006**, *364*, 309-322.

(44) Heroven, A. K.; Dersch, P. *Molecular Microbiology* **2006**, *62*, 1469-1483.

(45) Hernandez-Lucas, I.; Gallego-Hernandez, A. L.; Encarnacion, S.; Fernandez-Mora, M.; Martinez-Batallar, A. G.; Salgado, H.; Oropeza, R.; Calva, E. *Journal of Bacteriology* **2008**, *190*, 1658-1670.

(46) Ames, B. N. *Science* **1983**, *221*, 1256-1264.

(47) Choi, H. J.; Kim, S. J.; Mukhopadhyay, P.; Cho, S.; Woo, J. R.; Storz, G.; Ryu, S. E. *Cell* **2001**, *105*, 103-113.

(48) Storz, G.; Tartaglia, L. A.; Ames, B. N. *Science* **1990**, *248*, 189-194.

(49) Christman, M. F.; Storz, G.; Ames, B. N. *Proceedings of the National Academy of Sciences of the United States of America* **1989**, *86*, 3484-3488.

(50) Altuvia, S.; WeinsteinFischer, D.; Zhang, A. X.; Postow, L.; Storz, G. *Cell* **1997**, *90*, 43-53.

(51) Hwang, C.; Sinskey, A. J.; Lodish, H. F. *Science* **1992**, *257*, 1496-1502.

(52) Kullik, I.; Toledano, M. B.; Tartaglia, L. A.; Storz, G. *Journal of Bacteriology* **1995**, *177*, 1275-1284.

(53) Riddles, P. W.; Blakeley, R. L.; Zerner, B. *Analytical Biochemistry* **1979**, *94*, 75-81.
(54) Block, E.; Oconnor, J. *Journal of the American Chemical Society* **1974**, *96*, 3929-3944.
(55) Claiborne, A.; Miller, H.; Parsonage, D.; Ross, R. P. *Faseb Journal* **1993**, *7*, 1483-1490.
(56) Davis, F. A.; Jenkins, L. A.; Billmers, R. L. *Journal of Organic Chemistry* **1986**, *51*, 1033-1040.
(57) Tartaglia, L. A.; Gimeno, C. J.; Storz, G.; Ames, B. N. *Journal of Biological Chemistry* **1992**, *267*, 2038-2045.
(58) Toledano, M. B.; Kullik, I.; Trinh, F.; Baird, P. T.; Schneider, T. D.; Storz, G. *Cell* **1994**, *78*, 897-909.
(59) Christman, M. F.; Morgan, R. W.; Jacobson, F. S.; Ames, B. N. *Cell* **1985**, *41*, 753-762.
(60) Aslund, F.; Zheng, M.; Beckwith, J.; Storz, G. *Proceedings of the National Academy of Sciences of the United States of America* **1999**, *96*, 6161-6165.
(61) Seth, D.; Hausladen, A.; Wang, Y. J.; Stamler, J. S. *Science* **2012**, *336*, 470-473.
(62) Meuric, V.; Gracieux, P.; Tamanai-Shacoori, Z.; Perez-Chaparro, J.; Bonnaure-Mallet, M. *Oral Microbiology and Immunology* **2008**, *23*, 308-314.
(63) Diaz, P. I.; Slakeski, N.; Reynolds, E. C.; Morona, R.; Rogers, A. H.; Kolenbrander, P. E. *Journal of Bacteriology* **2006**, *188*, 2454-2462.
(64) Barnard, J. P.; Stinson, M. W. *Infection and Immunity* **1999**, *67*, 6558-6564.
(65) Amano, A.; Tamagawa, H.; Shizukuishi, S.; Tsunemitsu, A. *The Journal of Osaka University Dental School* **1986**, *26*, 187-92.
(66) Ohara, N.; Kikuchi, Y.; Shoji, M.; Naito, M.; Nakayama, K. *Microbiology-Sgm* **2006**, *152*, 955-966.
(67) Legrain, M.; Mazarin, V.; Irwin, S. W.; Bouchon, B.; Quentinmillet, M. J.; Jacobs, E.; Schryvers, A. B. *Gene* **1993**, *130*, 73-80.
(68) Kesavalu, L.; Holt, S. C.; Ebersole, J. L. *Oral Microbiology and Immunology* **2003**, *18*, 226-233.
(69) Marsh, P. D.; McDermid, A. S.; McKee, A. S.; Baskerville, A. *Microbiology-Uk* **1994**, *140*, 861-865.
(70) McKee, A. S.; McDermid, A. S.; Baskerville, A.; Dowsett, A. B.; Ellwood, D. C.; Marsh, P. D. *Infection and Immunity* **1986**, *52*, 349-355.
(71) Ueshima, J.; Shoji, M.; Ratnayake, D. B.; Abe, K.; Yoshida, S.; Yamamoto, K.; Nakayama, K. *Infection and Immunity* **2003**, *71*, 1170-1178.
(72) Sztukowska, M.; Bugno, M.; Potempa, J.; Travis, J.; Kurtz, D. M. *Molecular Microbiology* **2002**, *44*, 479-488.
(73) Elf, J.; Li, G. W.; Xie, X. S. *Science* **2007**, *316*, 1191-1194.
(74) Wang, A. C.; Revzin, A.; Butler, A. P.; Hippel, P. H. V. *Nucleic Acids Research* **1977**, *4*, 1579-1593.
(75) Li, G. W.; Xie, X. S. *Nature*, *475*, 308-315.
(76) Hellman, L. M.; Fried, M. G. *Nature Protocols* **2007**, *2*, 1849-1861.
(77) Chudakov, D. M.; Lukyanov, S.; Lukyanov, K. A. *Trends in Biotechnology* **2005**, *23*, 605-613.
(78) Tsien, R. Y. *Annual Review of Biochemistry* **1998**, *67*, 509-544.

(79) Drepper, T.; Eggert, T.; Circolone, F.; Heck, A.; Krauss, U.; Guterl, J. K.; Wendorff, M.; Losi, A.; Gartner, W.; Jaeger, K. E. *Nature Biotechnology* **2007**, *25*, 443-445.
(80) Lobo, L. A.; Smith, C. J.; Rocha, E. R. *Fems Microbiology Letters* **2011**, *317*, 67-74.